AD_____

Award Number: W81XWH-12-1-0250

TITLE: Therapeutic Role of Bmi-1 Inhibitors in Eliminating Prostate Tumor Stem Cells

PRINCIPAL INVESTIGATOR: Joseph Bertino, MD

CONTRACTING ORGANIZATION: Rutgers, The State University of New Jersey
NEW BRUNSWICK, NJ 08903-1914

REPORT DATE: October 2014

TYPE OF REPORT: Annual

PREPARED FOR: U.S. Army Medical Research and Materiel Command
Fort Detrick, Maryland 21702-5012

REPORT DOCUMENTATION PAGE

Form Approved
OMB No. 0704-0188

1. REPORT DATE	2. REPORT TYPE	3. DATES COVERED
October 2014	Annual	30 Sep 2013 - 29 Sep 2014

4. TITLE AND SUBTITLE

Therapeutic Role of Bmi-1 Inhibitors in Eliminating Prostate Tumor Stem Cells

5a. CONTRACT NUMBER

5b. GRANT NUMBER: W81XWH-12-1-0250

5c. PROGRAM ELEMENT NUMBER

6. AUTHOR(S)
Joseph Bertino, MD (Partnering PI),
Hatem E. Sabaawy, MD, PhD (Initiating PI),
Isaac Kim, MD, PhD (Partnering PI).

email: bertinoj@cinj.rutgers.edu

5d. PROJECT NUMBER

5e. TASK NUMBER

5f. WORK UNIT NUMBER

7. PERFORMING ORGANIZATION NAME (S) AND ADDRESS(ES)

Rutgers, The State University of New Jersey
NEW BRUNSWICK, NJ 08903-1914

8. PERFORMING ORGANIZATION REPORT NUMBER

9. SPONSORING / MONITORING AGENCY NAME(S) AND ADDRESS(ES)
U.S. Army Medical Research and Materiel Command
Fort Detrick, Maryland 21702-5012

10. SPONSOR/MONITOR'S ACRONYM(S)

11. SPONSOR/MONITOR'S REPORT NUMBER(S)

12. DISTRIBUTION / AVAILABILITY STATEMENT
Approved for Public Release; Distribution Unlimited

13. SUPPLEMENTARY NOTES

14. ABSTRACT

Current prostate cancer (PCa) management calls for identifying novel and more effective therapeutic approaches. Self-renewing prostate tumor-initiating cells (TICs) hold intrinsic therapy-resistance and account for tumor relapse and progression. BMI-1 (B-cell-specific MMLV insertion site-1) regulates stem cell self-renewal, thus, impairing BMI-1 function for TICs-tailored therapies appears to be a promising approach. During the first year of this award and in collaboration with the initiating and other partnering PIs, we developed a time-of-adherence assay to identify $CD49b^{hi}CD29^{hi}CD44^{hi}$ cells as TICs. This year, we identified the first known translational inhibitors of BMI-1; C-209 that target prostate TICs. Employment of this specific BMI-1 inhibitor on patient-derived cells significantly decreased spheroid formation *in vitro* and prevented tumor initiation *in vivo* in mice (Bertino Lab), thereby diminishing the frequency of TICs. Furthermore, C-209 induced prostate cancer cell senescence, and G1 cell cycle arrest. BMI-1 inhibition, while displaying antitumor activity in mouse xenografts did not exert toxic effects on normal tissues. BMI-1 targeted therapy when combined with taxotere resulted in further antitumor activities. These data offer a paradigm for targeting TICs for a more effective PCa treatment. Therefore, we have accomplished our second year's goal to demonstrate the beneficial effects of targeting prostate TICs *in vivo* in mice in this synergistic award between three laboratories (Sabaawy, Bertino, and Kim) to develop a therapeutic strategy for BMI-1 inhibitors in prostate cancer.

15. SUBJECT TERMS NOTHING LISTED

16. SECURITY CLASSIFICATION OF:			17. LIMITATION OF ABSTRACT	18. NUMBER OF PAGES	19a. NAME OF RESPONSIBLE PERSON
a. REPORT	b. ABSTRACT	c. THIS PAGE			USAMRMC
U	U	U	UU	73	19b. TELEPHONE NUMBER *(include area code)*

CONTENTS

Preprint of Bansal et al., *Nature Comm.*, in revision. (Manuscript, supplemental material and Editorial and peer review comments).

A. INTRODUCTION

We developed a combined immunophenotypic and time-of-adherence assay to identify human prostate TICs with increased BMI-1 expression. Our goal is to identify and subsequently develop a new class of bioavailable small molecules that inhibit tumor growth by selectively reducing BMI-1 production. The approved statement of work (SOW) described synergistic efforts of three laboratories; my laboratory: partnering-PI (Joseph Bertibo, MD; contract #W81XWH-12-1-0250); that of the initiating PI (Hatem Sabaawy, MD, PhD; contract #W81XWH-12-1-0249); and partnering-PI (Isaac Kim, MD, PhD; contract #W81XWH-12-1-0251) to ensure the achievement of this goal.

Three central elements are investigated in parallel in the three laboratories for this project; 1) Isolation and characterization of primary prostatectomy tissue (Kim Lab), 2) Drug screening for BMI-1 inhibitors utilizing zebrafish xenografts (Sabaawy Lab) and prostate cancer cell lines (Bertino Lab), and 3) Confirmation of the antitumor activity of C-209 in mouse xenografts alone and upon combination with taxotere (Bertino Lab).

The following tasks from **the approved SOW** were performed to achieve the goal of defining the strategy for use of effective BMI-1 inhibitors in future trials:
Task #1. Completed by Kim Lab.

Task #2. Models of primary prostate xenografts in mice (Bertino Lab). The TICs that were isolated from the Kim lab and given to us were examined for tumor growth characterization. Once mouse xenografts were established, treatment with C-209 resulted in a significant antitumor activity (See Figs. 7 of Bansal et al., *Nature Comm.* manuscript in revision that is attached in the Appendix).

Task #3. Completed by Sabaawy Lab.

Task #4. We examined antitumor effects of the BMI-1 inhibitor C-209 in mice and in combination therapy. (See Fig. 7e-g of Bansal et al., *Nature Comm.* manuscript in revision that is attached in the Appendix).

Task #5. We selected C-209 as the candidate BMI-1 inhibitor and examined *in vivo* effects in mice to confirm the in vivo zebrafish xenograft assays that were completed at the Sabaawy lab. The antitumor activities were in mice were similar to those found in zebrafish xenografts.

From the above experiments performed in the second year of the project, we have determined that C-209 is the BMI-1 inhibitor that was successfully used for *in vivo* studies in mice, and similar conclusions were achieved from zebrafish studies (Sabaawy Lab), therefore suggesting that this compound may be further pursued for PCa therapy. We have published one manuscript[1] from the studies of the first year and generated more data for the second manuscript (see appendix) on the characterization of the BMI-1 inhibitor C-209 that has been submitted to *Nature Comm.* and is currently under revision.

B. BODY (Experiments performed at the Bertino Lab)

Treatment of advanced prostate cancer (PCa) has been challenging with limited success[3]. Although several agents such as abiraterone, cabazitaxel, denosumab, sipuleucel-T became available during 2010 to 2014 for managing castration resistant PCa (CRPC), these therapies only marginally extend median survival by ~3 months[4,5], and resistance to these treatments are emerging. There is a dire need for therapies that are safe, efficacious, and cost-effective for treating CRPC, and can be used in early disease to prevent metastasis.

A fraction of PCa cells acquire and/or retain tumor initiation and self-renewal potentials, therefore termed TICs[6,7]. We have identified prostate TICs from primary tissues that are collagen-adherent $\alpha2\beta1^{hi}/CD44^{hi}$ cells[2]. Recent experimental and clinical studies have identified BMI-1 as a member of the polycomb family of chromatin remodeling complexes that act as transcriptional repressors for epigenetic chromatin modification. BMI-1 encodes a zinc finger protein that forms a key rate-limiting regulatory component of the polycomb repressor complex (PRC1) regulating cellular transcription. PRC1 enzymatic activities include DNA methylation of CpG islands and global mono-ubiquitination of histone 2A. Our data demonstrate that upregulated BMI-1 levels correlate with advanced PCa. PCa TICs can self-renew and also generate non-TIC progeny[6]. Prostate TICs survive treatment due to their intrinsic resistance to current therapies[8,9]. BMI-1 is a central player in PCa progression as it controls growth signals[10-15], regulates oncogenic microRNAs[16], and induces metastasis markers [17]. BMI-1 is overexpressed at levels much higher in cancer cells vs. normal cells[18], and contributes to therapy resistance, in particular in advanced and/or metastatic PCa[10,18,19]. Importantly, the strongest BMI-1 expression is observed in tissues[20,21], and plasma[22-25] of highly aggressive tumors undergoing metastasis. Notably, BMI-1 protein levels in serum of PCa patients correlate with increased serum PSA[26]. Therefore, BMI-1 is an excellent biomarker for advanced PCa, and targeting BMI-1 is a compelling therapeutic approach.

In the second year, we performed experiments to show that knockdown of BMI-1 inhibits cell proliferation and results in growth arrest (see Fig. 1 in Accomplished tasks). These data confirms the data generated from another group[11], whereas BMI-1 overexpression promotes anchorage independent growth and cell invasion[12]. With recent sequencing of pancreatic and kidney cancers[27,28] and determination of mutational landscape of PCa[29], an unexpected intratumor heterogeneity was revealed. A common feature of these heterogeneous clones is self-renewal, a feature that can be effectively targeted by inhibiting BMI-1.

We confirmed that primary PCa adherent $\alpha2\beta1^{hi}/CD44^{hi}$ TICs in mouse xenografts[2] overexpress BMI-1 (see accomplished tasks below; Fig. 1). TICs are comprised of heterogeneous subpopulations with multiple phenotypes[30]. Prostate TICs and invasive cells are enriched for CD44[31] (accomplished tasks; Fig. 2), suggesting an intriguing mechanism of initiating PCa invasion though basement membrane degrading activity of $CD44^{hi}$ TICs. In summary, BMI-1 is a critical target in PCa and developing BMI-1 inhibitors will provide novel and effective therapy for PCa treatment.

C. ACCOMPLISHED TASKS

Task1. Evaluation of BMI-1 expression in PCa.

This task was completed by the Kim Lab.

Task2. Isolation of prostate TICs using phenotypic and time-of-adherence assay. As compared to CSCs or TICs from other solid tumors, few studies have reported on the isolation of primary human prostate TICs, likely due to the limited availability of sizable primary tumor tissues. Our experimental approach allowed us to identify prostate TICs using a combination of time-of-adherence and phenotypic assays. We isolated $CD44^{hi}$ and $\alpha2\beta1$-$integrin^{hi}$ prostate TICs from prostatectomy tissues and PCa cell lines upon enrichment with collagen adherence[2].

On the basis of rapid adhesion on collagen, PCa cells were plated on a collagen-I dish for 5 min (5'=rapidly adherent) (3-5% of cells) were enriched for TICs by sorting the $\alpha_2\beta_1^{hi}/CD44^{hi}$ cells. The sorted adherent cells upregulated CD133 (From 0.01% to ~3%), and this fraction showed superior ability to form tumors in mice[2]. The $\alpha2\beta1^{hi}/CD44^{hi}$ cells have significantly higher colony forming efficiency, increased migration, and increased invasion abilities vs. $\alpha2\beta1^{low}/CD44^{low}$ cells[2]. The ability of the $\alpha2\beta1^{hi}/CD44^{hi}$ TICs to self-renew was tested in serial spheroid assays. Disaggregated primary spheroids from $\alpha2\beta1^{hi}/CD44^{hi}$ cells reformed spheroids in 2^{ry} and 3^{ry} assays, whereas those from $\alpha2\beta1^{low}/CD44^{low}$ cells formed only cell clusters in 2^{ry} assays, reflecting their limited stemness[2]. Thus, adherent $\alpha2\beta1^{hi}/CD44^{hi}$ cells are more tumorigenic *in vitro*, and in mice, therefore fulfilled the criteria of TICs.

Expression of CD44, α2β1-integrin, and CD133 in each fraction was analyzed. The 5 min-adherent cell fraction had an average of several fold higher number of cells highly coexpressing α2β1 and CD44 as compared to the 20 min-non-adherent in PC3 and CWR22 cells examined (Fig. 1). Thus phenotypically, the 5 min-adherent fraction is enriched in $\alpha2\beta1^{hi}/CD44^{hi}$ cells, while the 20 min-non-adherent fraction comprise $\alpha2\beta1^{low}/CD44^{low}$ cells. When cells from the 5 min-adherent fraction of PC3 and CWR22 cells that are $\alpha2\beta1^{hi}/CD44^{hi}$ cells were grown as prostate spheres, known to contain putative TICs that can initiate serially passageable spheres, the consistently low CD133 expression increased, and up to 5% of the cells were CD133, while CD133 was still undetectable in when grown as prostate spheres. Thus, we conclude that in primary prostate cancer cases, the 5 min-adherent fraction was enriched in $\alpha2\beta1^{hi}/CD44^{hi}$ cells, and in $CD133^{+}$ cells when grown as prostate spheres, compared to the non-adherent fraction.

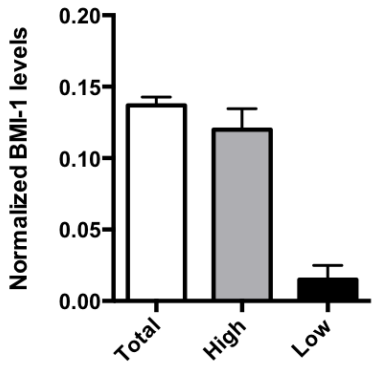

Figure 1. Expression of BMI-1 in diagnostic sections from prostate cancer patient. The CD49bhiCD29hiCD44hi cells have increased BMI-1 expression. Left, western Blot analysis of BMI-1 expression levels. Right, quantitation of BMI-1 expression levels from 3 independent experiments. Anti-tubulin was used as a loading control.

The TICs isolated from the Kim Lab by adherence to collagen. To evaluate BMI-1 involvement in: resistance to DNA damage-induced apoptosis, motility, invasiveness and clonogenecity (all cell features traced to the CSC subpopulation) I performed chemoresistance, clonogenecity and cell motility experiments on shRNA-mediated knockdown (Sh-SCR) and (sh-BMI-1) cells. The results are shown in Figure 2 suggested that knockdown of BMI-1 caused marked reduction in prostate cancer cell survival.

Task3. Evaluate BMI-1 inhibitors in targeting prosate TICs.

To determine if the 5 min-adherent cell fraction contains TICs, $\alpha2\beta1^{hi}/CD44^{hi}$ DU145 cells within this fraction were examined by colony formation, and migration and invasion assays. Cells within the 5 min-adherent cell fraction with an $\alpha2\beta1^{hi}/CD44^{hi}$ phenotype showed a nearly 2-fold higher colony formation, and increased migration and invasion abilities as compared to $\alpha2\beta1^{low}/CD44^{low}$ cells[2].

An essential characteristic of TICs is their ability to self-renew in serial plating assays. The $\alpha2\beta1^{hi}/CD44^{hi}$ DU145 cells formed significantly more single cell-derived spheroids as compared to $\alpha2\beta1^{low}/CD44^{low}$ cells. Moreover, spheroids formed from $\alpha2\beta1^{low}/CD44^{low}$ primary cells were fewer after day-5, and stopped growing after day-9 suggesting that these cells lack self-renewal abilities. To assess self-renewal at an earlier time point of sphere formation, single cells derived from day 7-primary spheroids were replated for secondary spheroid formation assays. Once again, $\alpha2\beta1^{hi}/CD44^{hi}$ primary cells generated significantly more spheroids than $\alpha2\beta1^{low}/CD44^{low}$ cells. Collectively, the $\alpha2\beta1^{hi}/CD44^{hi}$ prostate cancer cells exhibit enhanced tumorigenic, invasive, and self-renewal abilities.

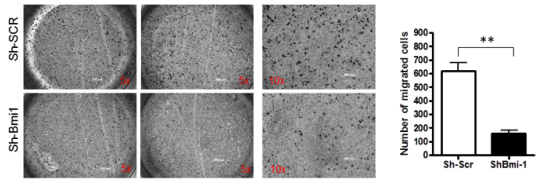

Figure 2. Effects of sh-RNA mediated targeting BMI-1. For migration assay, 20.000 Sh-SCR and sh-Bmi1 cells were plated in modified Boyden chambers and migratory capabilities were evaluated 96h later. For Chemosensitivity assay, 3000 cells were treated. After 96h, cell viability was evaluated by MTS assay. All experiments were performed in KSFM. Both experiments were performed twice with 4 replicates each.

TICs were shown to be resistant to chemotherapies. Since we isolated putative TICs by collagen adherence, we hypothesized that treatment with drugs that target TICs would reduce the number of cells adhering to collagen-I. Hence, we performed the collagen adherence assay upon treatment with chemotherapies commonly used for prostate cancer at IC_{50s} established by MTS assays. Indeed, the number of PCa collagen-adherent cells was not affected by chemotherapy treatments, and on the contrary increased with methotrexate (Fig. 3, left bars) suggesting that these agents that are frequently used in the clinic for cancer treatment might increase the percentage of putative TICs.

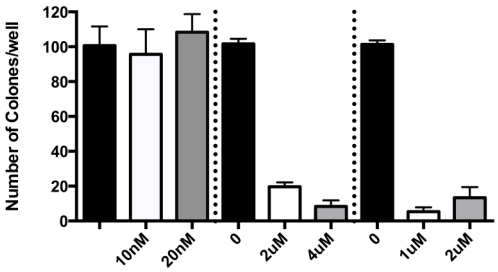

Figure 3. ***Effects of BMI-1 inhibitors vs. methotrexate (MTX) and doxorubicin on secondary and tertiary prostate spheroids formation from single cells.*** Bars from left to right; Methotrexate, C-209 and C-211. Rapidly adherent $CD49b^{hi}CD29^{hi}CD44^{hi}$ cells were plated on agarose-coated plates. The following day, cells were treated with methotrexate, doxorubicin, C-209 and C-211 at various concentrations for 72 hrs. Post-treatment, primary spheroids were collected, counted and single cell suspensions were plated on 6-well tissue culture dishes for secondary spheroid assays. After 14 days, the formed colonies were stained with crystal violet and counted as secondary spheroids, and displayed on the left as mean ± SD. For tertiary spheroids, single cells from day-7 secondary spheroids were separated, and methotrexate, C-209, and C-211 were added to the spheroids for 72 hrs. Post treatment, tertiary spheroids were stained with crystal violet and counted after 14 days. Data represent three independent experiments using IC_{50} concentrations (*), and 2x IC_{50} concentrations (**), and treatments were found to be statistically significant where indicated (*, **P<0.005 compared to untreated).

An essential property of TICs is their ability to initiate tumor growth in immune-compromised mice with limited cell numbers. We tested whether the 5 min-adherent primary PCa cells are more tumorigenic. Cells were injected SC in the abdominal flanks of nude mice. Tumors were analyzed by three variables: tumor incidence, tumor growth rate (mm^3/day), and final tumor volume $(mm^3)^2$. Only 17% of mice (n=3/20) injected with non-adherent cells developed tumors, while nearly all mice injected with either adherent (n=18/20) (90%) or total cells (n=17/20) (85%) developed tumors. Thus, the $\alpha2\beta1^{hi}/CD44^{hi}$ DU145 cells are more tumorigenic in mice. Tumors were allowed to grow until they reached the size of ~100 mm^3, then mice were treated with C-209 or the chemotherapeutic agent docetaxel for 2 weeks (Fig. 4). At the end of treatments, while vehicle-treated tumors grew exponentially and docetaxel appeared to exert an effect on xenografts growth, only C-209-treated tumors were significantly inhibited (Fig. 4). Additionally, since tumor relapse is frequently observed following treatment discontinuation, tumor volume was constantly monitored with an electronic caliper for additional 10 days. Noticeably, the results in Fig. 4, while revealing a significant difference in tumor growth between docetaxel-treated and untreated mice, shown an even higher disparity in

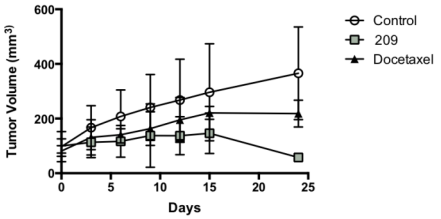

Figure 4. ***Activity of BMI-1 inhibitor in mouse PCa xenografts.*** C-209 effectively inhibited BMI-1 production in tumor tissues *in vivo*. PCa cells were implanted SC in NSG mice and, after tumor development, mice were randomized and administered C-209 SC at a dose of 60 mg/kg/day for ten days. Treatment with C-209 significantly inhibited tumor growth (n=8 mice /group, ***p<0.002).

C-209-treated xenografts compared to controls thus, corroborating the efficiency of anti-BMI-1-based therapy. Severe tumor damage indicated by the large necrotic areas and scarce cellularity observed in these tumors was present two weeks after the last delivery of chemotherapy and BMI-1 inhibitors. These data suggest that the BMI-1 inhibitor C-209 displays significant antitumor activity in mouse xenografts of PCa.

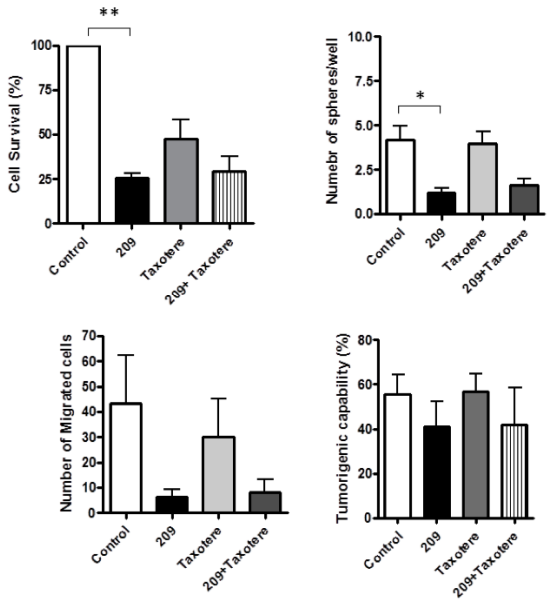

Figure 5. Comparing the effects of C-209 and taxotere. Patient-derived PCa cells were treated with Taxotere and 209, alone or combined, for 3 days. On day 3 cells were collected, counted by Trypan Blue exclusion and replated in fresh medium without treatments for additional 4 days. Cell viability at day 4 (Top left) clonogenic capability at day 21 (Top right), number of migrated cells (bottom left) and tumorigenic ability (bottom right) were evaluated. The total number of patients analyzed in these graphs was seven.

Task4. Drug discovery of BMI-1 inhibitors. To investigate if pharmacological targeting of BMI-1 would provide a potential therapy to target prostate TICs, we screened a small molecule library (from PTC Therapeutics) for inhibitors of BMI-1 utilizing both luciferase- and GFP-reporters encompassing the 5`UTR and 3`UTR of BMI-1[32]. These small molecules selectively bind to BMI-1 mRNA, and modulate post-transcriptional expression of BMI-1 protein [32]. They were selected based on their 3-D chemical structure[32], and were synthesized by Rutgers chemistry group for clinical applications. After screening hundreds in zebrafish (Sabaawy Lab) and cell reporter assays, compounds with superior kinetics, toxicity, and efficacy in BMI-1 knockdown were identified. The IC_{50} values were determined using MTT assays. The Sabaawy lab used fish embryonic toxicology assays to show that selected compounds have no toxicity *in vivo*, and do not affect embryonic ESCs. Toxicology assays allowed us to select a number of small molecules for further testing (C-209). This small molecule inhibited the expression of BMI-1 in primary cells, with the expected reduction in downstream ubiquitinated γ-H2A levels. Following treatment withdrawal, the percentage of primary PCa cells able to survive with either treatment appears to be statistically reduced in C-209 alone similar to combination with taxotere (Fig. 5). The same results were obtained in soft agar assays performed to evaluate differences in colony forming abilities (Fig. 5). No statistical significance was observed migration or tumorigenic capabilities of cells following treatments of C-209 alone compared to the combination with taxotere. Final conclusion of theses data require additional assays in more primary cells to increase statistical power These studies are going to be completed during the third year of this award.

In **SUMMARY**, we confirmed our recently published data[2] for identification of TICs in additional primary PCa tissues. We have examined a number of prostate cancer patients with adenocarcinomas and showed that BMI-1/CD44 correlate in high-grade histological and clinical prostate cancer. We confirmed the activity of C-209 in mouse xenografts and further confirmed these findings in secondary assays of cells dissociated from these xenografts. We will continue to study the roles of BMI-1 in targeting TICs in primary PCa[2] and mouse xenografts, and develop a defined rational for combination therapies during the third year of this project.

D. KEY RESEARCH ACCOMPLISHMENTS

- We developed a combined immunophenotypic and time-of-adherence assay to identify human prostate tumor initiating cells (TICs). These studies were recently published.

- We recruited 19 patients with prostate adenocarcinoma, and found increased BMI-1 expression in cancer tissues compared to the adjacent normal tissues. These studies will continue with additional patients' tissues in the next year.

- Utilizing primary PCa cells and mouse xenograft model, we identified the first known translational inhibitors of BMI-1 that target prostate TICs. The BMI-1 inhibitor C-209 induced prostate cancer cell senescence, and G1 cell cycle arrest.

- Targeting of BMI-1 with C-209 in prostate cancer significantly reduced clonogenic, migration, and invasion abilities of TICs, and increased cellular senescence.

- Treatment of mouse xenografts with the BMI-1 inhibitor C-209 reduced the clonogenic, migration, and invasion potentials of PCa cells in secondary assays from cells dissociated from treated xenografts.

- These data support a paradigm of therapeutically targeting TICs in prostate cancer with C-209.

E. REPORTABLE OUTCOMES

A second manuscript from this award:

Bansal N, Bartucci M, Yussuf S, Davis S, Flaherty K, Huselid E, Cao L, Sydorenko N, Moon Y Zhong H, Stein MN, Kim IY, Davis T, DiPaola RS, Bertino JR, Sabaawy HE. **Selective BMI-1 targeting interferes with tumor-initiating cell survival and tumor growth in prostate cancer**. Nature Comm. (Under revision). (Manuscript, supplemental material and Editorial and peer review comments are attached in the appendix).

F. CONCLUSION

Prostate tumor-initiating cells (TICs) have intrinsic resistance to current therapies. BMI-1 (B-cell-specific MMLV insertion site-1) regulates stem cell self-renewal, and is over-expressed in TICs. We developed a combined immunophenotypic and time-of-adherence assay to identify human prostate TICs with increased BMI-1 expression. Tumor initiation and dissemination were consistently observed in the immune-permissive NSG mice microenvironment, generating a model for primary prostate adenocarcinomas. Utilizing the mouse xenograft model, we identified the first known translational inhibitors of BMI-1 that target prostate TICs. BMI-1 inhibitors induced prostate cancer cell senescence, and G1 cell cycle arrest. Targeting of BMI-1 significantly reduced clonogenic, migration, and invasion abilities of TICs, and increased cellular senescence. Treatment of mouse xenografts with the BMI-1 inhibitor C-209 inhibited tumor growth and was additive when combined with taxotere in mouse xenografts. Therefore, we have accomplished our goal to demonstrate the beneficial effects of targeting prostate TICs with BMI-1 inhibitors during the second year of this project. This work also resulted in a publication demonstrating our ability to isolate and propagate primary prostate cancer TICs during the first year and a second manuscript submitted to Nature Communications. The next phase of studies will further examine the roles of BMI-1 targeted therapy in prostate cancer from additional primary tissues, and specifically examine the value of combining TICs-targeted therapy using BMI-1 inhibitors with common therapies targeting the bulk of prostate cancer such as taxotere from prostatectomy tissues in order to develop a therapeutic strategy for prostate cancer treatment by the completion of the project.

G. REFERENCES

1. Luo J, Zha S, Gage WR, Dunn TA, Hicks JL, Bennett CJ, Ewing CM, Platz EA, Ferdinandusse S, Wanders RJ, Trent JM, Isaacs WB, De Marzo AM. Alpha-methylacyl-CoA racemase: a new molecular marker for prostate cancer. Cancer Res 62:2220-6, (2002). PMC: 11956072.

2. Bansal N, Davis S, Tereshchenko I, Budak-Alpdogan T, Zhong H, Stein MN, Kim IY, DiPaola RS, Bertino JR, Sabaawy HE. Enrichment of human prostate cancer cells with tumor initiating properties in mouse and zebrafish xenografts by differential adhesion. Prostate, Oct 24. doi: 10.1002/pros.22740. [Epub ahead of print] (2013). PMC: 24154958.

3. Jin JK, Dayyani F, Gallick GE. Steps in prostate cancer progression that lead to bone metastasis. Int J Cancer 128:2545-61, (2011). PMC: 21365645.

4. Dayyani F, Gallick GE, Logothetis CJ, Corn PG. Novel therapies for metastatic castrate-resistant prostate cancer. J Natl Cancer Inst 103:1665-75, (2011). PMC: 21917607.

5. MacVicar GR, Hussain MH. Emerging therapies in metastatic castration-sensitive and castration-resistant prostate cancer. Curr Opin Oncol 25:252-60, (2013). PMC: 23511665.

6. Collins AT, Berry PA, Hyde C, Stower MJ, Maitland NJ. Prospective identification of tumorigenic prostate cancer stem cells. Cancer Res 65:10946-51, (2005). PMC: 16322242.

7. Guo C, Zhang B, Garraway IP. Isolation and characterization of human prostate stem/progenitor cells. Methods Mol Biol 879:315-26, (2012). PMC: 22610567.

8. Ramaswamy S, Ross KN, Lander ES, Golub TR. A molecular signature of metastasis in primary solid tumors. Nat Genet 33:49-54, (2003). PMC: 12469122.

9. Danila DC, Heller G, Gignac GA, Gonzalez-Espinoza R, Anand A, Tanaka E, Lilja H, Schwartz L, Larson S, Fleisher M, Scher HI. Circulating tumor cell number and prognosis in progressive castration-resistant prostate cancer. Clin Cancer Res 13:7053-8, (2007). PMC: 18056182.

10. Fan C, He L, Kapoor A, Gillis A, Rybak AP, Cutz JC, Tang D. Bmi1 promotes prostate tumorigenesis via inhibiting p16(INK4A) and p14(ARF) expression. Biochim Biophys Acta 1782:642-8, (2008). PMC: 18817867.

11. Fasano CA, Dimos JT, Ivanova NB, Lowry N, Lemischka IR, Temple S. shRNA knockdown of Bmi-1 reveals a critical role for p21-Rb pathway in NSC self-renewal during development. Cell Stem Cell 1:87-99, (2007). PMC: 18371338.

12. Song LB, Li J, Liao WT, Feng Y, Yu CP, Hu LJ, Kong QL, Xu LH, Zhang X, Liu WL, Li MZ, Zhang L, Kang TB, Fu LW, Huang WL, Xia YF, Tsao SW, Li M, Band V, Band H, Shi QH, Zeng YX, Zeng MS. The polycomb group protein Bmi-1 represses the tumor suppressor PTEN and induces epithelial-mesenchymal transition in human nasopharyngeal epithelial cells. J Clin Invest 119:3626-36, (2009). PMC: 19884659.

13. Dimri GP, Martinez JL, Jacobs JJ, Keblusek P, Itahana K, Van Lohuizen M, Campisi J, Wazer DE, Band V. The Bmi-1 oncogene induces telomerase activity and immortalizes human mammary epithelial cells. Cancer Res 62:4736-45, (2002). PMC: 12183433.

14. Liu S, Dontu G, Mantle ID, Patel S, Ahn NS, Jackson KW, Suri P, Wicha MS. Hedgehog signaling and Bmi-1 regulate self-renewal of normal and malignant human mammary stem cells. Cancer Res 66:6063-71, (2006). PMC: 16778178.

15. Jacobs JJ, Kieboom K, Marino S, DePinho RA, van Lohuizen M. The oncogene and Polycomb-group gene bmi-1 regulates cell proliferation and senescence through the ink4a locus. Nature 397:164-8, (1999). PMC: 9923679.

16. Cao Q, Mani RS, Ateeq B, Dhanasekaran SM, Asangani IA, Prensner JR, Kim JH, Brenner JC, Jing X, Cao X, Wang R, Li Y, Dahiya A, Wang L, Pandhi M, Lonigro RJ, Wu YM, Tomlins SA, Palanisamy N, Qin Z, Yu J, Maher CA, Varambally S, Chinnaiyan AM. Coordinated regulation of polycomb group complexes through microRNAs in cancer. Cancer Cell 20:187-99, (2011). PMC: 21840484.

17. Yang MH, Hsu DS, Wang HW, Wang HJ, Lan HY, Yang WH, Huang CH, Kao SY, Tzeng CH, Tai SK, Chang SY, Lee OK, Wu KJ. Bmi1 is essential in Twist1-induced epithelial-mesenchymal transition. Nat Cell Biol 12:982-92, (2010). PMC: 20818389.

18. Glinsky GV. Death-from-cancer signatures and stem cell contribution to metastatic cancer. Cell Cycle 4:1171-5, (2005). PMC: 16082216.

19. Berezovska OP, Glinskii AB, Yang Z, Li XM, Hoffman RM, Glinsky GV. Essential role for activation of the Polycomb group (PcG) protein chromatin silencing pathway in metastatic prostate cancer. Cell Cycle 5:1886-901, (2006). PMC: 16963837.

20. van Leenders GJ, Dukers D, Hessels D, van den Kieboom SW, Hulsbergen CA, Witjes JA, Otte AP, Meijer CJ, Raaphorst FM. Polycomb-group oncogenes EZH2, BMI1, and RING1 are overexpressed in prostate cancer with adverse pathologic and clinical features. Eur Urol 52:455-63, (2007). PMC: 17134822.

21. Cooper CS, Campbell C, Jhavar S. Mechanisms of Disease: biomarkers and molecular targets from microarray gene expression studies in prostate cancer. Nat Clin Pract Urol 4:677-87, (2007). PMC: 18059348.

22. Silva J, Garcia V, Garcia JM, Pena C, Dominguez G, Diaz R, Lorenzo Y, Hurtado A, Sanchez A, Bonilla F. Circulating Bmi-1 mRNA as a possible prognostic factor for advanced breast cancer patients. Breast Cancer Res 9:R55, (2007). PMC: 17711569.

23. Xu W, Zhou H, Qian H, Bu X, Chen D, Gu H, Zhu W, Yan Y, Mao F. Combination of circulating CXCR4 and Bmi-1 mRNA in plasma: A potential novel tumor marker for gastric cancer. Mol Med Rep 2:765-71, (2009). PMC: 21475899.

24. Zhang X, Wang C, Wang L, Du L, Wang S, Zheng G, Li W, Zhuang X, Dong Z. Detection of circulating Bmi-1 mRNA in plasma and its potential diagnostic and prognostic value for uterine cervical cancer. Int J Cancer 131:165-72, (2011). PMC: 21858805.

25. Tong YQ, Liu B, Zheng HY, He YJ, Gu J, Li F, Li Y. BMI-1 autoantibody as a new potential biomarker for cervical carcinoma. PLoS One 6:e27804, (2011). PMC: 22132147.

26. Siddique HR, Parray A, Zhong W, Karnes RJ, Bergstralh EJ, Koochekpour S, Rhim JS, Konety BR, Saleem M. BMI1, stem cell factor acting as novel serum-biomarker for Caucasian and African-American prostate cancer. PLoS One 8:e52993, (2013). PMC: 23308129.

27. Campbell PJ, Yachida S, Mudie LJ, Stephens PJ, Pleasance ED, Stebbings LA, Morsberger LA, Latimer C, McLaren S, Lin ML, McBride DJ, Varela I, Nik-Zainal SA, Leroy C, Jia M, Menzies A, Butler AP, Teague JW, Griffin CA, Burton J, Swerdlow H, Quail MA, Stratton MR, Iacobuzio-Donahue C, Futreal PA. The patterns and dynamics of genomic instability in metastatic pancreatic cancer. Nature 467:1109-13, (2010). PMC: 20981101.

28. Gerlinger M, Rowan AJ, Horswell S, Larkin J, Endesfelder D, Gronroos E, Martinez P, Matthews N, Stewart A, Tarpey P, Varela I, Phillimore B, Begum S, McDonald NQ, Butler A, Jones D, Raine K, Latimer C, Santos CR, Nohadani M, Eklund AC, Spencer-Dene B, Clark G, Pickering L, Stamp G, Gore M, Szallasi Z, Downward J, Futreal PA, Swanton C. Intratumor heterogeneity and branched evolution revealed by multiregion sequencing. N Engl J Med 366:883-92, (2012). PMC: 22397650.

29. Barbieri CE, Bangma CH, Bjartell A, Catto JW, Culig Z, Gronberg H, Luo J, Visakorpi T, Rubin MA. The mutational landscape of prostate cancer. Eur Urol 64:567-76, (2013). PMC: 23759327.

30. Magee JA, Piskounova E, Morrison SJ. Cancer stem cells: impact, heterogeneity, and uncertainty. Cancer Cell 21:283-96, (2012). PMC: 22439924.

31. Patrawala L, Calhoun T, Schneider-Broussard R, Li H, Bhatia B, Tang S, Reilly JG, Chandra D, Zhou J, Claypool K, Coghlan L, Tang DG. Highly purified CD44+ prostate cancer cells from xenograft human tumors are enriched in tumorigenic and metastatic progenitor cells. Oncogene 25:1696-708, (2006). PMC: 16449977.

32. Cao L, Bombard J, Cintron K, Sheedy J, Weetall ML, Davis TW. BMI1 as a novel target for drug discovery in cancer. J Cell Biochem, (2011). PMC: 21678481.

H. APPENDIX

Preprint of manuscript and supplemental data:

Bansal N, Bartucci M, Yussuf S, Davis S, Flaherty K, Huselid E, Cao L, Sydorenko N, Moon Y Zhong H, Stein MN, Kim IY, Davis T, DiPaola RS, Bertino JR, Sabaawy HE. **Selective BMI-1 targeting interferes with tumor-initiating cell survival and tumor growth in prostate cancer**. *Nature Comm.* (Under revision). (Manuscript, supplemental material and Editorial and peer review comments are attached in the appendix).

Selective BMI-1 targeting interferes with tumor-initiating cell survival and tumor growth in prostate cancer

Nitu Bansal[1§], Monica Bartucci[1§], Shamila Yusuff[1], Stephani Davis[2], Kathleen Flaherty[1], Eric Huselid[2], Liangxian Cao[3], Nadiya Sydorenko[3], Young-Choon Moon[3], Hua Zhong[4], Daniel J. Medina[1,5], Mark N. Stein[1,5], Isaac Y. Kim[1,6], Thomas W. Davis[3], Robert S. DiPaola[1,5], Joseph R. Bertino[1,2,5*], Hatem E. Sabaawy[1,2,5*]

[1]Rutgers Cancer Institute of New Jersey, Rutgers University, New Brunswick, NJ 08901.
[2]Department of Pharmacology, RBHS-Robert Wood Johnson Medical School, Graduate School of Biomedical Sciences, Rutgers University, New Brunswick, NJ 08901.
[3]PTC Therapeutics, Inc., 100 Corporate CT, South Plainfield, NJ 07080.
Departments of [4]Pathology and Laboratory Medicine, [5]Medicine and [6]Surgery, RBHS-Robert Wood Johnson Medical School, Rutgers University, New Brunswick, NJ 08901.

[§] These authors contributed equally.
*Corresponding authors:
J R Bertino, M.D.
Cancer Institute of New Jersey, 195 Little Albany Street, Room 3033, New Brunswick, NJ 08901, USA. Telephone: 732-235-8510
Email address: bertinoj@cinj.rutgers.edu

H E Sabaawy, M.D., Ph.D.
Cancer Institute of New Jersey, 195 Little Albany Street, Room 4557, New Brunswick, NJ 08901, USA. Telephone: 732-235-8081
Email address: sabaawhe@cinj.rutgers.edu

Running Title: BMI-1 targeting in tumor-initiating cells

Key words: Prostate cancer stem cells, tumor-initiating cells, BMI-1, zebrafish

Text word count: 4,344

Abstract word count: 150

ABSTRACT

Current prostate cancer (PCa) management calls for identifying novel and more effective therapeutic approaches. Self-renewing tumor-initiating cells (TICs) hold intrinsic therapy-resistance and account for tumor relapse and progression. BMI-1 regulates stem cell self-renewal, thus, impairing BMI-1 function for TICs-tailored therapies appears to be a promising approach. We have previously developed a combined immunophenotypic and time-of-adherence assay to identify $CD49b^{hi}CD29^{hi}CD44^{hi}$ cells as human prostate TICs. Here we show that in TICs, BMI-1 expression is upregulated and associated with stem cell-like traits. Employment of a specific BMI-1 inhibitor on patient-derived tumor cells significantly decreased spheroid formation *in vitro* and prevented tumor initiation *in vivo*, thereby functionally diminishing the frequency of TICs. Furthermore, BMI-1 inhibition, while displaying antitumor activity in both zebrafish and mouse xenografts, did not exert toxic effects on normal tissues. These data offer a paradigm for targeting TICs and support the development of BMI-1-related therapy for more effective PCa treatment.

INTRODUCTION

Prostate cancer (PCa) is the most commonly diagnosed cancer and the sixth leading cause of cancer-related death among men worldwide [1]. Current treatments, especially in the advanced disease, are only temporarily effective with the inevitable development of therapy resistance and relapse [2,3], making the prognosis for these patients bleak [4]. Others and we have shown that primary PCa tissues contain tumor cells endowed with self-renewal and tumorigenic potential [5-10] that are known as tumor-initiating cells (TICs). Compelling evidence indicates that TICs account for tumor initiation, maintenance and progression [11]. Additionally, by the virtue of their resistance to therapy, TICs have been proposed to be the cause of tumor relapse. Thus, in order to accomplish tumor eradication, efforts are made to design TIC-tailored therapeutic approaches that would selectively target these highly aggressive tumorigenic cells.

An attractive treatment strategy is to use agents that are able to impede the self-renewal abilities of TICs, and can therefore target heterogeneous TICs within a given patient [12]. BMI-1 (B-cell specific MMLV insertion site-1), a member of the polycomb family of chromatin remodeling complex, was shown to regulate stem cell self-renewal including the normal prostate and play a key role in PCa initiation and progression [13,14]. In clinical specimens, increased BMI-1 expression was found to be associated with adverse pathologic features, including high rates of PCa recurrence [15]. Moreover, microarray analyses showed that genetic components and downstream targets of the polycomb pathway are associated with therapy-resistant PCa [16]. Altogether, these data closely associate BMI-1 with the presence of tumor-initiating stem-like cells in clinical PCa samples. Under these circumstances, it is reasonable to assume that small-molecule

inhibitors that target BMI-1 could be the first in a new class of antitumor therapy specifically directed against self-renewing and chemo-resistant TICs.

Previously, we have developed a surrogate self-renewal assay that allowed us to isolate prostate TICs from PCa tissue based on α2β1-integrin (also called CD49b/CD29) and CD44 protein expression [10]. Herein, we investigated the role of BMI-1 in human prostate TICs. We demonstrate that in prostate TICs, BMI-1 is overexpressed and functionally regulating their survival and maintenance. Targeting of BMI-1 with a novel translational inhibitor impaired self-renewal and migratory potential *in vitro* without affecting normal stem cell viability. Consistent with these *in vitro* data, BMI-1 inhibition *in vivo* decreased tumor growth and was associated with a significant reduction of TICs in patient-derived samples and tumor xenografts as evaluated by CD49b/CD29/CD44 staining, serial transplantation *in vivo* and clonogenic assays from xenografts-derived cells *ex-vivo.* Remarkably, these latter outcomes were not observed following conventional chemotherapy treatments. Given the role of TICs in the clinical PCa scenario, these observations support the evaluation of BMI-1 inhibitors for more effective PCa treatments.

RESULTS

BMI-1 is a potential target for human prostate TICs

BMI-1 has been suggested to be a key player in PCa initiation, recurrence and progression [14,15]. In line with this notion, when we evaluated BMI-1 expression in normal prostate cells compared to a series of different PCa cell lines, BMI-1 was expressed in the latter, but was low to undetectable in normal prostate epithelial cells (Supplementary Fig. 1a). To assess the functional role(s) of BMI-1 in PCa development, we performed loss-of-function analyses of BMI-1 in DU145 PCa cells (Supplementary Fig. 1b). Importantly, downregulation of BMI-1 was associated with decreased cell motility, decreased clonogenic capability and chemoresistance (Supplementary Fig. 1c-e). Of note, resistance to drug-induced apoptosis, motility, invasiveness and clonogenicity have been traced to TICs [17]. We recently found that in PCa, clonogenic, migratory and tumorigenic potentials are enriched in the rapidly adherent $CD49b^{hi}CD29^{hi}CD44^{hi}$ cell population [10].

Therefore, in an attempt to evaluate a possible correlation between TICs and BMI-1-driven self-renewal that could be used for therapeutic purposes, we analyzed BMI-1 expression in both the rapidly adherent $CD49b^{hi}CD29^{hi}CD44^{hi}$ and non-adherent $CD49b^{low}CD29^{low}CD44^{low}$ PCa cells. We found that in the $CD49b^{hi}CD29^{hi}CD44^{hi}$ phenotype, BMI-1 is significantly overexpressed when compared to the $CD49b^{low}CD29^{low}CD44^{low}$ cells (Fig. 1a), thus indicating that BMI-1 is predominantly present in the tumorigenic cell compartment of PCa. To study whether BMI-1 expression modulates the levels of rapidly adherent $CD49b^{hi}CD29^{hi}CD44^{hi}$ cells, we employed the collagen adherence assay after lentiviral-mediated knockdown of BMI-1.

Loss of BMI-1 in DU145 cells resulted in a significant (>50%) decrease in the numbers of rapidly adherent cells when compared with control scrambled-shRNA-treated cells (Fig. 1b), thus suggesting that BMI-1 has an impact on TICs population expansion.

Identification of pharmacological BMI-1 inhibitors

Since knockdown of BMI-1 decreased the numbers TICs, we searched for small molecule inhibitors of BMI-1 using the collagen adherence and MTS assays. High-throughput screening against a library composed of >200,000 small molecules (PTC Therapeutics) was performed in reporter cells that contains the luciferase open reading frame flanked with the human BMI-1 5'- and 3'-UTRs to identify BMI-1 translational inhibitors [18]. Seven translational inhibitors of BMI-1 expression with the same core chemical structure (Fig. 1c) were found to target the post-transcriptional control mechanisms that act through the 5` or 3`UTR of BMI-1 mRNA in luciferase assays [18,19]. To examine the antitumor activity of these compounds, we first determined their IC_{50} concentrations in DU145 cells (Supplementary Fig. 2a). Among them, three compounds: C-209, C-210 and C-211 significantly decreased the number of collagen-adherent cells by an average of 30-50% (Fig. 1d). Furthermore, in treated cells, BMI-1 inhibition was confirmed to be dose-dependent (Fig. 1e-f).

BMI-1 knockdown was shown to induce senescence [13]. Thus, to further validate the specificity of action of these compounds, mouse embryonic fibroblasts (MEFs), that are either Bmi-$1^{+/+}$ or Bmi-$1^{-/-}$, were treated with C-209, C-210 and C-211 respectively and β-gal staining was assessed to evaluate senescence levels. While C-209, C-210,

and C-211 treatments elicited a significant increase in senescence of the Bmi-$1^{+/+}$ MEFs compared to untreated cells, these effects, as expected, were not significant in the highly senescent Bmi-$1^{-/-}$ MEFs (Supplementary Fig. 2b-c). Moreover, knockdown of BMI-1 using shRNA resulted in a significant increase in senescence of DU145 cells (Supplementary Fig. 2b-c) further validating the senescence-specific effects of the BMI-1 inhibitors.

Pharmacological targeting of BMI-1 in human prostate TICs

To confirm that BMI-1 inhibition had activity against the putative TIC fraction in PCa, we treated DU145, PC3 and CWR22 PCa cells with C-209. This treatment significantly impaired the percentage of rapidly adherent $CD49b^{hi}CD29^{hi}CD44^{hi}$ cells (Fig. 2a-b), most likely by selectively targeting BMI-1, as collectively elucidated by a G1 cell cycle arrest (Supplementary Fig. 2d), as expected from loss of BMI-1 cell cycle regulatory function(s) [18], complemented by a reduced S phase (Supplementary Fig. 2d), and a dose-dependent reduction in both BMI-1 protein level and C-terminal lysine-119 mono-ubiquitinated form of γ-H2A, a specific product of the BMI-1 PRC1 complex activity [20] (Supplementary Fig. 2f). Additionally, C-209 selectivity was further validated by lack of significant inhibition of a panel of 160 kinase and 21 phosphatase (data not shown).

Self-renewal capacity is a distinguishing property of stem cells [21]. Thus, clonogenic assays have been developed to estimate the frequency and the properties of TICs within a given tumor, especially after treatments [22]. To evaluate the ability of these

compounds to target serial clonogenic capacity, single cells collected from 7 days cultured primary spheroids were plated on low attachment plates in the presence of C-209, C-211, methotrexate, and doxorubicin, the latter are two commonly used therapeutic agents. Consequently, the secondary spheroids were counted, dissociated and replated to determine their serial colony forming potential. In contrast to the slight inhibitory effects of methotrexate and doxorubicin, treatment with C-209 significantly diminished the number of single cell-derived colonies in secondary spheroid assays (Fig. 2c). More importantly, the outcomes of C-209 and C-211 treatment on tertiary colony formation were remarkable, as nearly a 10-fold reduction was observed, while methotrexate had no effect (Fig. 2c). Overall, these results suggested that inhibiting BMI-1 might eliminate self-renewing cells in PCa.

Effects of BMI-1 inhibition on normal stem cells

An important concern in the use of stem cell inhibitors is the effect of these compounds on normal stem cell compartments when they are used to target TICs. The zebrafish embryo is a valuable tool for investigating vertebrate developmental toxicity and it is emerging as an alternative model for *in vivo* drug toxicity screening [23,24].

In zebrafish, the *bmi-1a* gene and a second paralog named *bmi-1b* share respectively an 80% and 76% amino acid sequence homology with the human BMI-1 [25]. Thus, we performed toxicological assays of the selected compounds in zebrafish embryos. In particular, we investigated whether pharmacological inhibition of *bmi-1* might interfere with zebrafish embryonic stem cell development. In 24- and 48-hour

developmental assays, C-209, C210, and C-211 had no toxic effects on zebrafish embryonic development at their respective IC_{50s} (Fig. 3a). However, unlike C-209, both C-210 and 211 exhibited adverse pharmacokinetic properties at later time points (data not shown). Furthermore, when used at high doses, C-210 and C-211 severely impeded embryo hatching at 48-hours, and demonstrated higher toxicity and embryo curling suggesting non-linear kinetics (Fig 3a). On the contrary, zebrafish embryonic stem cell development and survival was not impacted in C-209-treated embryos (Fig. 3b). Furthermore, bathing of zebrafish embryos in C209-additioned water caused a dose-dependent reduction in zebrafish bmi-1a and bmi-1b protein levels (Fig. 3c). Altogether these data prompted us to dismiss C-210 and 211 inhibitors and focus our investigations on the C-209 inhibitor with a safe toxicity profile.

To further confirm the lack of C-209 toxicity on normal tissue stem cells, we treated primary human $CD34^+$ hematopoietic stem cells (HSCs) with the BMI-1 inhibitor and analyzed colony formation after 2 weeks. Treatment with C-209 at the IC_{50} concentration (2 μM) did not affect hematopoietic clonogenic capacity, but drastically reduced DU145 PCa colony formation (Fig. 3d). Thus validating the zebrafish assays and suggesting that targeting BMI-1 might have selective role(s) in inhibiting clonogenic potential of tumor stem-like cells compared to normal cells.

BMI-1 inhibition in patient-derived TICs

To assess the value of a new treatment, primary patient-derived cells represent a much more relevant experimental tool compared to standard cancer cell lines. Despite the known difficulties in culturing primary PCa cells *in vitro*, even if for brief periods, we

have recently successfully maintained primary PCa cells endowed with self-renewal and tumorigenic potential in culture [10]. Therefore, we sought to determine a possible future therapeutic role of BMI-1 inhibitors by testing treatment with C-209 compound (Fig. 4a) in a panel of primary PCa cells (Table 1). BMI-1 inhibition in patient-derived PCa cells resulted in significant antitumor activity at an IC_{50} lower but not significantly different from that of DU145 cells (Fig. 4b). Notably, as previously observed with tumor cell lines, treatment with C-209 caused an important reduction in the CD49b/CD29/CD44 population in primary PCa cultures (Fig. 4c). Remarkably, treatment with docetaxel, an indicated first line chemotherapy treatment for advanced PCa, resulted in enrichment of the highly aggressive $CD49b^{hi}CD29^{hi}CD44^{hi}$ cells.

The effectiveness of any therapeutic strategy is based on the chemosensitivity of the tumor, the presence of minimal residual disease post chemotherapy treatments and especially on the absence of relapse and/or secondary clonally derived lesions [26]. Since TICs account for tumor spread and relapse by the virtue of their treatment-resistance, self-renewal and tumor-seeding capacity [17], it is reasonable to deduce that the efficacy of a TIC-tailored strategy is based on a diminished clonogenic and tumorigenic capacity.

In order to evaluate C-209 efficiency in targeting patient-derived TICs, we initially treated distinct primary PCa cells for four consecutive days with either C-209 or docetaxel. Subsequently, in order to investigate the long-term impact of treatments, particularly in a post therapy discontinuation setting, cells were washed to remove the treatment compounds and replated. Cell rescue and soft agar assays were assessed to evaluate differences in cell survival and colony-forming repopulation abilities.

Interestingly, both docetaxel and C-209 treatments impaired short-term survival of primary PCa, although the latter to a more significant extent (Fig. 4d). Nevertheless and more critically, patient-derived PCa cells maintained the ability to form colonies after single treatments with docetaxel but not after C-209 treatment (Fig. 4e), indicating that BMI-1 inhibition impairs survival and clonogenic activity of primary PCa TICs.

BMI-1 has been implicated in cancer metastasis in a variety of tumor types including PCa [27]. As previously indicated, we also observed that loss of function of BMI-1 in PCa cell lines led to impaired cell migration (Supplementary Fig. 1c). To evaluate whether or not primary PCa cells would respond to BMI-1 inhibition with decreased cell motility, we assessed the propensity of patient-derived PCa cells to migrate in modified Boyden chambers. We found that, upon C-209 treatment, PCa cells diminish their motility (Fig. 4f). In contrast, docetaxel–treated cell migratory potential was almost unchanged when compared to controls (Fig. 4f), thus confirming a possible role of BMI-1 in cancer dissemination.

Evaluation of BMI-1 inhibitors *in vivo*

Successful murine xenografting of primary human PCa, in the absence of inducing murine urogenital mesenchyme [28], has rarely been reported. We have previously shown that both embryonic and juvenile zebrafish can be successfully used as xenograft models of primary human PCa [10]. Here, we employed a model designed to identify small molecule inhibitors that functionally target BMI-1 and self-renewal activities (Fig. 5a). We first isolated PCa cells from seventeen patients undergoing surgical

prostatectomy (Table 1), and examined their tumor initiation potential in zebrafish xenografts. Prostate cancers were diagnosed based on histological examination (Fig. 5b-d) and loss of basal cell markers compared to adjacent PIN and normal tissues (data not shown). As we recently demonstrated [10], the expression of the PCa-specific alpha-methylacyl coenzyme-A racemase (AMACR) when combined with overexpression of Erg [29], resulting from PCa cells harboring the TMPRSS2-Ets fusion, provide excellent dual PCa-specific biomarkers [10] (Fig. 5e-g and Supplementary Fig. 3a-b). We detected Erg overexpression associated with AMACR in the mirror sections of sampled PCa tissue (Fig. 5e-g), and upon formation of TIC-derived zebrafish xenografts (Supplementary Fig. 3e) in cells that expressed the human isoform of CD44 and BMI-1 (Supplementary Fig. 3f-h). TICs isolated from primary prostate adenocarcinoma engrafted robustly in the pre-immune zebrafish embryos (Fig. 5h). Histological analyses demonstrated xenograft tumor formation (Fig. 5h-k) with cells that appear to have similar morphology to the patient's biopsy cells (compare cells in Fig. 5d to those in Fig. 5k) and that were positive for Prostatic Specific Antigen (PSA) staining (Fig. 5l-o) confirming their prostatic origin.

Initially, we employed the zebrafish embryo *in vivo* drug toxicity assay to confirm that the compounds and chemotherapies under investigation when used at IC_{50} concentrations have no notable toxicities (Supplementary Fig. 4). To study whether or not C-209 had also antitumor activity, we injected zebrafish embryo with small numbers of quantum dot (QD)-labeled TICs isolated from both cell lines and primary PCa tissues (Fig. 6a and Supplementary Fig. 5a). As low as ten QD-labeled TICs were able to initiate tumors (Figure 6a). Treatment of these embryos with C-209 at 2 μM led

to tumor shrinkage (Fig. 6b and supplementary Fig. 5b, left and right panels) from multiple patient samples (Fig. 6c). Likewise, treatment of juvenile xenograft fish with the BMI-1 inhibitor C-209 led to tumor reduction (Supplementary Fig. 5c, left and right panels) indicating that, although governing the cell fate of TICs, BMI-1 likely regulates the viability of PCa in general.

Nevertheless, to determine the BMI-1 inhibitor efficacy in targeting the tumorigenic compartment of the tumor, primary PCa were treated with either docetaxel or C-209 for several days. Subsequently, cells were washed to remove the treatment compounds, injected into zebrafish embryos and tumor appearance was monitored. Notably, after 10 days C-209 treated cells gave rise to a significantly lower number of tumors when compared to either control or docetaxel-treated cells (Fig. 6d), thus indicating that BMI-1 inhibition diminishes the tumorigenic cell population in PCa samples. Notably, these effects were associated with a significant reduction in Ki67 staining (Fig. 6e).

Xenotransplantation, followed by serial repopulation, is considered as an essential criterion to assess serial maintenance of stemness in defining TICs. Thus, to further examine if C-209 halts tumor initiation and/or self-renewal of primary PCa cells in zebrafish xenografts, we sorted labeled tumor cells from primary zebrafish xenografts that were either treated with DMSO or C-209, and used them for secondary xenografts (Fig. 6f). TICs from DMSO-treated embryos were able to initiate secondary xenografts in 81.8% of cases (n=54/66 secondary xenograft embryo from three patient samples), while C-209-treated cells had significantly less tumor initiation potential since they were only able to initiate secondary xenografts in 29.3% of cases (n=22/75 secondary

xenograft embryo from three patient samples) ($p<0.001$) (Fig. 6f), giving the proof-in-principle that BMI-1 targeting therapy is effectively impairing the frequency of TICs. Moreover, because we observed that BMI-1 is affecting cell motility potential *in vitro*, and to evaluate whether BMI-1 is directly involved in the metastatic process *in vivo*, we performed histological analyses on localized and metastatic tumor sections of zebrafish xenografts. Primary xenograft masses, identified through the specific cell expression of human CD44[10], had <50% of cells expressing BMI-1, in contrast to >90% of cells expressing BMI-1 in metastatic colonies (Fig. 6g-h). These data suggest that metastatic tumors might contain a larger fraction of TICs and/or metastasis initiating cells expressing BMI-1 and that BMI-1 might play a prominent role in cancer dissemination.

Zebrafish provide a powerful model organism to study tumor self-renewal and for cancer drug discovery [30]. Nevertheless, we do recognize that not enough evidence support the notion that the zebrafish model can displace the use of a mammalian model system such as the mouse. Thus, in order to confirm whether C-209 treatment affected tumor response and TIC survival in a murine model, we produced xenograft tumors derived from human rapidly adherent $CD49b^{hi}CD29^{hi}CD44^{hi}$ TICs [10] into NOD-SCID-IL-2R null (NSG) mice and employed a strategy aimed at unraveling the targeting of self-renewing TICs (Fig.7a). Tumors were allowed to grow until they reached the size of ~100 mm^3, then mice were treated with C-209 or the chemotherapeutic agent docetaxel for 2 weeks (Fig. 7b). At the end of treatments, while vehicle-treated tumors grew exponentially and docetaxel appeared to exert an effect on xenografts growth, only C-209-treated tumors were

significantly inhibited (Fig. 7b). Additionally, since tumor relapse is frequently observed following treatment discontinuation, tumor volume was constantly monitored with an electronic caliper for additional 10 days. Noticeably, the results in Fig. 7b, while revealing a significant difference in tumor growth between docetaxel-treated and untreated mice, shown an even higher disparity in C-209-treated xenografts compared to controls thus, corroborating the efficiency of anti-BMI-1-based therapy. Severe tumor damage indicated by the large necrotic areas and scarce cellularity observed in these tumors was present two weeks after the last delivery of chemotherapy and BMI-1 inhibitors (Fig. 7c). In line with this, ki67+ cells in grafts with reduced nuclear BMI-1 and surface CD44 expression from anti- BMI-1 treated mice were significantly lower when compared vehicle-treated tumors (Fig. 7d-e), demonstrating the anti-proliferative activity of C-209 in mouse PCa xenografts.

Nevertheless, given that in treated tumors, the number of clonogenic cells should parallel the number of tumorigenic cells, to investigate whether C-209 treatment was able to target TICs in mouse tumors, a clonogenic assay *in vitro* and a serial transplantation *in vivo* were assessed using cells dissociated from treated and untreated xenografts (Fig. 7a). Interestingly, the clonogenic potential of cells dissociated from C-209 treated tumors was significantly impaired as compared to controls (Fig. 7f), and their graft repopulation potential was reduced (Fig. 7g), thus demonstrating that BMI-1 targeting is effective against the pool of tumor-propagating cells.

Altogether, our data demonstrate that C-209 is a novel small molecule translational inhibitor of BMI-1 that displays mutually effective anti-TICs and antitumor activities in both zebrafish and mouse xenografts.

DISCUSSION

Mounting evidence points to a distinct subpopulations of cancer stem cells (CSCs) or TICs as responsible for tumor generation and treatment failure. Although the CSCs concept is still object of controversies [17,31], evidence supporting key role(s) of TICs in tumor initiation and recurrence has been strengthened by a number of lineage tracing studies [32-34]. Accordingly, it is evident that in order to achieve tumor eradication, we need new approaches that are able to target the tumorigenic core of cancers. TICs are tumor cells that possess indefinite replicative ability due to an inherent self-renewal potential. In the context of a tumor, though, even mutated transit-amplifying cells can acquire or enhance their self-renewal capacity [35-37]. Moreover, self-renewal abilities might also be dynamically changing and/or evolving [11,38] during the clonal selection process [37]. Consequently, targeting self-renewal potential of a given tumor cell populations may be the key to develop more effective anticancer drugs [38]. BMI-1 is a key component of a transcriptional repressor complex that plays important roles in cell cycle regulation and cellular senescence principally by repressing $p16^{INK4a}$/$p19^{ARF}$-regulatory functions [39]. Furthermore, it is an important regulator of stem cell self-renewal and maintenance [40,41].

In PCa, activation of BMI-1 was detected in primary mouse xenografts [27], transgenic mouse prostate tumors [14,42] and in stem cell fractions from advanced metastatic PCa with unfavorable prognosis [16]. Additionally, the expression of BMI-1 in samples from PCa patients with moderate Gleason scores was highly predictive of PSA recurrence [15]. BMI-1 thus is a critical target for inhibiting the proliferative activities of prostate TICs and PCa overall.

To validate our assumption, we initially employed a genetic approach to show that knockdown of BMI1 transcript levels impairs stem cell-like traits in PCa cells most likely by reducing TICs frequency. To verify our assumption, we identify, through a high-throughput screening platform, a small molecule BMI-1 inhibitor and investigate its ability to interfere with CSCs survival and self-renewal capacity. Human prostate spheroids have increased levels of BMI-1 [43]. Herein we showed that similarly in the $CD49b^{hi}CD29^{hi}CD44^{hi}$ tumorigenic stem-like cells, BMI-1 expression levels are higher and functional when compared to the non-tumorigenic counterpart. Colony and serial spheroid formation and tumor xenograft studies show that BMI-1 controls self-renewal, hence tumor-seeding capacity of $CD49b^{hi}CD29^{hi}CD44^{hi}$ prostate cells. Of note, the same outcomes were not observed upon treatments with conventional anticancer agents such as methotrexate, doxorubicin or docetaxel. Notably, molecular and/or pharmacological targeting of BMI-1 impairs TIC-associated features alongside with survival of PCa cells in general, as shown by the antitumor activity displayed by C-209 inhibitor in zebrafish and mouse PCa xenografts. ChIP-Seq and global mapping analyses revealed a complex network of BMI-1 targets, with almost 1,600 BMI-1-targeted gene, coding for proteins involved in the apoptosis and cell survival pathways, independent of BMI-1's classical $p16^{INK4a}/p19^{ARF}$- regulatory functions [44]. These data are consistent with the proliferation-promoting function of BMI-1, confirming that BMI-1 acts partly by preventing apoptosis and cell cycle arrest [45], and explain the anti-proliferative effects observed following BMI-1 inhibition in our study.

A possible drawback for the development of agents targeting stem cell self-renewal may be the potential toxicity deriving from inhibition of pathways used by normal tissue stem

cells [46]. Importantly, C-209 had less of an effect on $CD34^+$ HSCs, and no toxicity developed in zebrafish embryos, or during mice treatment at the IC_{50} concentration. These findings suggest that it might be possible to target tumor-initiating cells overexpressing BMI-1, without notable toxic effects on normal stem cells development, although this finding needs to be further verified.

Tumor regrowth is often observed in cancer patients following chemotherapy withdrawal. We found that the interruption of C-209 treatment did not correspond with a rapid rebound in tumor growth, suggesting that administration of BMI-1 inhibitors could be exploited to devise more effective therapeutic approaches for PCa. Importantly, the significant reduction in the number of clonogenic cells in tumor xenografts treated with C-209 and the reduced serial transplantation capacity of xenograft-derived cells, suggests that such treatment affects the survival of TICs, which are largely spared by treatment with docetaxel. BMI-1 may also cooperate with other factors such as TWIST1 to regulate the epithelial-to-mesenchymal transition (EMT) [47], a state associated with CSCs and metastasis. In line with this notion, we found that BMI-1 is overexpressed in secondary tumor lesions and that BMI-1 inhibition is accompanied by a reduced cell motility capacity in PCa suggesting a relationship between BMI-1 expression, highly self-renewing TICs and cancer dissemination in PCa.

Multiple molecular pathways regulate the biology of stem cells and are therefore potential targets in TICs [48]. Among these interacting pathways are BMI-1, OCT3/4, Hedgehog (Hh), Wnt/β-catenin, Notch signaling, Hox gene family, PTEN/Akt pathway, efflux transporters such as ABCG markers of self-renewal, and upregulated telomerase activity [49]. Studies suggest that BMI-1 is necessary for Hh-[50], and β-catenin-mediated

self-renewal [51] making BMI-1 most critical among these self-renewal targets [52]. A comprehensive analysis of pathways activated by BMI-1 inhibition in $CD49b^{hi}CD29^{hi}CD44^{hi}$ cells conducted by reverse-phase proteomic arrays showed interaction of multiple pathways (M.B. and H.S., manuscript in preparation), suggesting that a network of signals contributes to BMI-1-mediated effects. Additional studies are currently under way to delineate the effects of BMI-1 inhibitors on these other important stem cell regulators.

Many experimental studies rely on the use of immortalized cell lines that do not span the range of PCa phenotypes and may not be representative of the original tumors. We therefore generated patient-derived cultures and developed a zebrafish xenograft model of tumor initiation [10] that allowed us to identify inhibitors targeting BMI-1. We believe that such a model will be ideal for developing strategies to address tumor heterogeneity and identifying additional inhibitors targeting this or other self-renewal pathways for use in mono or combination therapy and precision medicine approaches [26]. In this regard, the use of primary tumor samples in our model might provide a platform for appropriate clonal, drug and dose selection for combination therapies.

In summary, through cell-based and zebrafish xenograft assays, we identified the first known small molecule inhibitors of BMI-1 that target prostate TICs. Furthermore, *in vivo* outcomes were confirmed in the mammalian mouse xenograft system. We conclude that BMI-1 is a bonafide target for development of drugs impeding "stemness" and overall survival in prostate cancer. Taken together, these observations support the clinical evaluation of BMI-1 inhibitors for a more effective treatment of PCa.

MATERIALS AND METHODS

Materials

Bmi-1 inhibitors were from PTC therapeutics; South Plainfield, NJ. Docetaxel (also called taxotere), doxorubicin, and methotrexate were from Rutgers Cancer Institute of New Jersey (CINJ) pharmacy. Collagen-I was purchased from BD Biosciences, and NOD/SCID/IlRγ mice were from the Jackson laboratory.

Collagen adherence assay

Putative cancer stem-like cells or TICs were isolated by combining phenotypic analyses [5] with collagen adherence as previously described [10]. Briefly, tissue culture dishes were coated with 70 μg/ml of collagen-I for 1 hr at room temperature or overnight at 4°C. Plates were washed with PBS, blocked in 0.3% BSA for 30 minutes, washed again, and cells were plated on collagen for 5 minutes or 20 minutes. Cells that adhere in 5 minutes, and cells that did not adhere after 20 minutes were collected, and used for further experiments.

Identification of BMI-1 translational inhibitors

We have examined a small molecule library (PTC therapeutics) for inhibitors of BMI-1 utilizing luciferase reporters encompassing the 5`UTR and 3`UTR of human BMI-1 [18]. The anti-BMI-1 antibody clone F6 was used for ELISA assays and for western blotting to examine the levels of BMI-1. The principal BMI-1's downstream target, mono-ubiquitinated (u) histone H2A, was examined using a mouse monoclonal anti-ubiquityl-histone H2A antibody (clone E6C5) (Millipore). The selectivity of C-209 was further investigated by profiling it against both a library of purified protein kinase targets using

the Z'-LYTE SelectScreen profiling activity assay (Invitrogen) against 245 kinases at [ATP] Km and [C-209] of 3 μM determinations, and a phosphatase profiler assay with an IC_{50} profiler (Millipore). Both assays yielded <10% activity for C-209.

Cell culture

Primary PCa cells were isolated from PCa specimens obtained at Rutgers Cancer Institute of New Jersey in accordance with an IRB-approved protocol and upon informed consent from patients undergoing surgical resection. All procedures were carried according to the Institutional Review Board (IRB) guidelines. Following surgical specimen dissociation, recovered cells were cultured in prostate epithelial basal media (PrEBM, Lonza). Cells from immortalized PCa lines were maintained at low passage numbers in minimal essential media (MEM) (GIBCO), 10% fetal bovine serum, and 1% penicillin-streptomycin. TICs, obtained from DU145 cells after selection, were maintained in keratinocyte serum free medium supplemented with epidermal growth factor (EGF) and bovine pituitary extract (KSFM media) (All from Invitrogen).

Flow cytometry

For cytofluorimetric analysis, PCa cells were collected, washed in 1xPBS, 2% FBS and 0.01% sodium azide and stained with anti-CD44-APC (Miltenyi) and anti-CD49b/CD29-FITC (BD). Cells were also stained with isotype controls, and with 7AAD to exclude dead cells. The effects of C-209 treatment on the expression of CD44 and CD49b/CD29 were assayed in DU145, PC3 and CWR22 cells treated for 72 hrs. Acquisition were made using a BD FACSCalibur flow cytometer (Becton Dickinson, Franklin Lakes, NJ) and

analysed using cell quest software.

Western blot

For western blot analysis, 50μg of whole cell lysates were used. Nitrocellulose membranes were incubated with mouse monoclonal anti-Bmi-1 clone F6 against the N-terminal (1:1000) (Millipore), rabbit polyclonal anti-Bmi-1 SDI against the C-terminal (1:2,000) and rabbit polyclonal anti-β-actin (1:10,000) (Rockland). Densitometric analysis was performed using Scion Image (Scion Corporation, Frederick, MO) and all results were normalized over β-actin.

Colony forming ability assay

For colony forming abilities, collagen-I-adherent cells at 5 minutes and non-adherent cells after 20 minutes were suspended at 2 x 10^3 cells/well in KSFM media. Every 3 days, half of the media was replaced and spheroids consisting of >50 cells were counted on day14. Single cells from day-7 spheroids were used in secondary and tertiary spheroid assays. Colony forming abilities of prostate cancer cells plated at 1 x 10^3 cells/well in six-well dishes coated with 1% agar were done as described [53,54]. Metotrexate, doxobicine, C-209 and C-211 were used at the indicated concentrations.

Soft agar colony forming assays were carried out for primary PCa cells treated with docetaxel and C-209 for 96h. Subsequently, cells were washed and 500 single cells were plated in the top agar layer in each well of a 24-well culture plate with 0.3% top agar layer and 0.4% bottom agar layer (SeaPlaque Agarose, Cambrex, NJ). Cultures were incubated at 37°C for 20 days. Colonies from triplicate wells were stained with crystal violet (0.01% in 10% MetOH), visualized and counted under microscope and photographed.

To obtain xenograft-derived cells, tumors were aseptically removed and dissociated. Cells recovered were extensively washed; subsequently 500 cells for each treatment condition were plated as described above. After 20 days, colonies were visualized and counted as described above.

$CD34^+$ colony forming assay

$CD34^+$ cells were isolated from cord blood samples (Elie Katz umbilical cord blood banking center, NJ) using MACS magnetic column separation system (Miltenyi). Briefly, cells were magnetically labeled with $CD34^+$ microbeads, and run twice through magnetic columns to increase purity. Cell viability and purity were assessed by flow cytometry. Purified $CD34^+$ cells were supplemented with IL-3, rhTPO (Kirin brewery), and FLT3-L (Peprotech) cytokines. Cells were suspended at 3 x 10^3 concentration in one ml of methocult (Methocult GF H4434; Stem cell technologies). Colonies were enumerated over a period of 2 weeks.

Cell survival assays. Primary PCa cells were treated with docetaxel or C-209 for 4 days. On day 4 cells were collected, washed and replated in fresh medium without in the absence of treatments for additional 4 days. On day 8 cells were collected and counted by Trypan Blue exclusion.

Migration assay

Cell migration was assessed in 24-well transwell Boyden chambers (Costar Scientific Corporation, Cambridge, MA). Single cells ($2x10^4$) were suspended in a complete growth

medium and placed into upper chambers. After 24 hrs incubations, migrated cells were stained with Coomassie Brilliant Blue and counted under the microscope.

Labeling, transplantation and treatment of PCa grafts in zebrafish

Wild type EKK and AB* zebrafish (*Danio rerio*) were maintained following an approved animal protocol. Adult fish were spawned and reared in conditioned water at 28.5°C on a 14-h light-10-h dark cycle. Embryos were staged as described (http://zfin.org). To track human PCa cells in embryos and juvenile Casper [55] fish, cells were labeled with QDs that are virtually resistant to photobleaching as described [10]. Following initial imaging, transplanted embryos were maintained at 33°C for up to 12 days. Juvenile zebrafish at 6-8 weeks of age were immune-suppressed with 10 μg/ml dexamethazone for 2 days as previously described [56,57], and were utilized for generating xenografts. For primary PCa, cells were allowed to adhere to collagen, sorted for $CD49b^{hi}CD29^{hi}CD44^{hi}$ expression, and subfractions were transplanted into zebrafish embryos. Embryos and juveniles were treated with the different compounds dissolved in a final concentration of 0.1-1% of DMSO in embryo water in 96- or 24-well plates. Xenografts were examined for QD fluorescence upon tumor formation and/or treatment, and sections were fixed, cut and stained with IHC as previously described [10].

Treatment of mouse xenografts

DU145 cells were implanted subcutaneously in NSG mice. After tumor formation, mice were randomized and administered twice with docetaxel 6 mg/kg and C-209 SC at a dose of 60 mg/kg/day for twelve days. Tumor growth was evaluated with an electronic caliper

before every administration. To evaluate drug efficacy, tumors were allowed to grow in the absence of treatment and measured every 3 days until day 24 and subsequently removed. Immunohistochemistry was performed on formalin fixed paraffin-embedded tissues. Paraffin sections (5μm) were incubated with anti-Ki67 (Upstate-Millipore, Billerica, MA), -BMI-1 (Clone 6, Millipore) and -CD44 (R&D Systems). Slides were counterstained with eosin. Percentage of Ki67 positive cells in mouse and zebrafish tumor xenografts was assessed by counting five different fields in each slide derived from two independent experiments. To calculate retention of tumor-seeding capacity, following treatments, tumor xenografts were dissociated and equal number of cells reinjected into secondary recipient mice or zebrafish.

Statistical analysis. All statistical analyses were performed using GraphPad Prism 6 (GraphPad Software Inc., www.graphpad.com). Data are presented as mean ± standard deviation (SD). Statistical significance was determined by student's t-test or ANOVA (one-way or two-way) with Bonferroni post-hoc test. A P value <0.05 is represented by a single asterisk, a P value <0.01 is represented by a double asterisk, while three asterisks indicate $P<0.001$, unless otherwise indicated.

ACKNOWLEDGEMENTS

We thank Drs. Maarten van Lohuizen (The Netherlands Cancer Institute) and Shridar Ganesan (Cancer Institute of New Jersey) for the Bmi-1 knockout Mouse Embryonic Fibroblasts (MEFs), and Leonard Zon (Harvard) for the Casper zebrafish. This project has been funded by the Department of Defense Prostate Cancer Grant (W81XWH-12-1-0249 to H.S.), National Cancer Institute (P30 CA072720 to R.D.), Rutgers Cancer Institute of New Jersey (Pilot Grant to J.B. and H.S.) and in part by Wellcome Trust grant (SDDI award # 092687) awarded to PTC therapeutics Inc.

AUTHORS CONTRIBUTIONS

1. Conception and design – Nitu Bansal, Monica Bartucci, Hatem E. Sabaawy, Joseph R. Bertino

2. Provision of study material or patient samples – Liangxian Cao, Nadiya Sydorenko, Young-Choon Moon, Thomas W. Davis, Mark N. Stein, Isaac Yi Kim

3. Collection and assembly of data – Nitu Bansal, Monica Bartucci, Shamila Yusuff, Stephani Davis, Kathleen Flaherty, Eric Huselid, Hatem E. Sabaawy

4. Data analysis and interpretation – Nitu Bansal, Monica Bartucci, Hatem E. Sabaawy, Robert DiPaola, Joseph R. Bertino

5. Manuscript writing – Monica Bartucci, Hatem E. Sabaawy

REFERENCES

1. Siegel, R., Naishadham, D. & Jemal, A. Cancer statistics, 2013. *CA Cancer J Clin* **63**, 11-30 (2013).

2. Dayyani, F., Gallick, G.E., Logothetis, C.J. & Corn, P.G. Novel therapies for metastatic castrate-resistant prostate cancer. *J Natl Cancer Inst* **103**, 1665-1675 (2011).

3. MacVicar, G.R. & Hussain, M.H. Emerging therapies in metastatic castration-sensitive and castration-resistant prostate cancer. *Curr Opin Oncol* **25**, 252-260 (2013).

4. Tannock, I.F.*, et al.* Docetaxel plus prednisone or mitoxantrone plus prednisone for advanced prostate cancer. *N Engl J Med* **351**, 1502-1512 (2004).

5. Collins, A.T., Berry, P.A., Hyde, C., Stower, M.J. & Maitland, N.J. Prospective identification of tumorigenic prostate cancer stem cells. *Cancer Res* **65**, 10946-10951 (2005).

6. Goldstein, A.S.*, et al.* Trop2 identifies a subpopulation of murine and human prostate basal cells with stem cell characteristics. *Proc Natl Acad Sci U S A* **105**, 20882-20887 (2008).

7. Toivanen, R.*, et al.* Brief report: a bioassay to identify primary human prostate cancer repopulating cells. *Stem Cells* **29**, 1310-1314 (2011).

8. Qin, J.*, et al.* The PSA(-/lo) prostate cancer cell population harbors self-renewing long-term tumor-propagating cells that resist castration. *Cell Stem Cell* **10**, 556-569 (2012).

9. Hoogland, A.M.*, et al.* Validation of stem cell markers in clinical prostate cancer: alpha6-integrin is predictive for non-aggressive disease. *Prostate* **74**, 488-496 (2014).

10. Bansal, N.*, et al.* Enrichment of human prostate cancer cells with tumor initiating properties in mouse and zebrafish xenografts by differential adhesion. *Prostate* **74**, 187-200 (2014).

11. Kreso, A. & Dick, J.E. Evolution of the cancer stem cell model. *Cell Stem Cell* **14**, 275-291 (2014).

12. Liu, W.*, et al.* Copy number analysis indicates monoclonal origin of lethal metastatic prostate cancer. *Nat Med* **15**, 559-565 (2009).

13. Park, I.K.*, et al.* Bmi-1 is required for maintenance of adult self-renewing haematopoietic stem cells. *Nature* **423**, 302-305 (2003).

14. Lukacs, R.U., Memarzadeh, S., Wu, H. & Witte, O.N. Bmi-1 is a crucial regulator of prostate stem cell self-renewal and malignant transformation. *Cell Stem Cell* **7**, 682-693 (2010).

15. van Leenders, G.J.*, et al.* Polycomb-group oncogenes EZH2, BMI1, and RING1 are overexpressed in prostate cancer with adverse pathologic and clinical features. *Eur Urol* **52**, 455-463 (2007).

16. Glinsky, G.V. Death-from-cancer signatures and stem cell contribution to metastatic cancer. *Cell Cycle* **4**, 1171-1175 (2005).

17. Visvader, J.E. & Lindeman, G.J. Cancer stem cells in solid tumours: accumulating evidence and unresolved questions. *Nat Rev Cancer* **8**, 755-768 (2008).

18. Cao, L.*, et al.* BMI1 as a novel target for drug discovery in cancer. *J Cell Biochem* (2011).

19. Peltz, S.W., Welch, E.M., Trotta, C.R., Davis, T. & Jacobson, A. Targeting post-transcriptional control for drug discovery. *RNA Biol* **6**, 329-334 (2009).

20. Chagraoui, J., Hebert, J., Girard, S. & Sauvageau, G. An anticlastogenic function for the Polycomb Group gene Bmi1. *Proc Natl Acad Sci U S A* **108**, 5284-5289 (2011).

21. Lajtha, L.G. Stem cell concepts. *Differentiation* **14**, 23-34 (1979).

22. Franken, N.A., Rodermond, H.M., Stap, J., Haveman, J. & van Bree, C. Clonogenic assay of cells in vitro. *Nat Protoc* **1**, 2315-2319 (2006).

23. Sipes, N.S., Padilla, S. & Knudsen, T.B. Zebrafish: as an integrative model for twenty-first century toxicity testing. *Birth Defects Res C Embryo Today* **93**, 256-267 (2011).

24. Selderslaghs, I.W., Blust, R. & Witters, H.E. Feasibility study of the zebrafish assay as an alternative method to screen for developmental toxicity and embryotoxicity using a training set of 27 compounds. *Reprod Toxicol* **33**, 142-154 (2012).

25. Le Faou, P., Volkel, P. & Angrand, P.O. The zebrafish genes encoding the Polycomb repressive complex (PRC) 1. *Gene* **475**, 10-21 (2011).

26. Sabaawy, H.E. Genetic Heterogeneity and Clonal Evolution of Tumor Cells and their Impact on Precision Cancer Medicine. *J Leuk (Los Angel)* **1**, 1000124 (2014).

27. Berezovska, O.P.*, et al.* Essential role for activation of the Polycomb group (PcG) protein chromatin silencing pathway in metastatic prostate cancer. *Cell Cycle* **5**, 1886-1901 (2006).

28. Risbridger, G.P. & Taylor, R.A. Minireview: regulation of prostatic stem cells by stromal niche in health and disease. *Endocrinology* **149**, 4303-4306 (2008).

29. Chaux, A.*, et al.* Immunohistochemistry for ERG expression as a surrogate for TMPRSS2-ERG fusion detection in prostatic adenocarcinomas. *Am J Surg Pathol* **35**, 1014-1020 (2011).

30. White, R., Rose, K. & Zon, L. Zebrafish cancer: the state of the art and the path forward. *Nat Rev Cancer* **13**, 624-636 (2013).

31. Rosen, J.M. & Jordan, C.T. The increasing complexity of the cancer stem cell paradigm. *Science* **324**, 1670-1673 (2009).

32. Driessens, G., Beck, B., Caauwe, A., Simons, B.D. & Blanpain, C. Defining the mode of tumour growth by clonal analysis. *Nature* **488**, 527-530 (2012).

33. Chen, J.*, et al.* A restricted cell population propagates glioblastoma growth after chemotherapy. *Nature* **488**, 522-526 (2012).

34. Schepers, A.G.*, et al.* Lineage tracing reveals Lgr5+ stem cell activity in mouse intestinal adenomas. *Science* **337**, 730-735 (2012).

35. Hemmati, H.D.*, et al.* Cancerous stem cells can arise from pediatric brain tumors. *Proc Natl Acad Sci U S A* **100**, 15178-15183 (2003).

36. Singh, S.K.*, et al.* Identification of a cancer stem cell in human brain tumors. *Cancer Res* **63**, 5821-5828 (2003).

37. Nowell, P.C. The clonal evolution of tumor cell populations. *Science* **194**, 23-28 (1976).

38. Visvader, J.E. & Lindeman, G.J. Cancer stem cells: current status and evolving complexities. *Cell Stem Cell* **10**, 717-728 (2012).

39. Jacobs, J.J.*, et al.* Bmi-1 collaborates with c-Myc in tumorigenesis by inhibiting c-Myc-induced apoptosis via INK4a/ARF. *Genes Dev* **13**, 2678-2690 (1999).

40. Melotti, A.*, et al.* In vitro and in vivo characterization of highly purified human mesothelioma derived cells. *BMC Cancer* **10**, 54 (2010).

41. Grinstein, E. & Wernet, P. Cellular signaling in normal and cancerous stem cells. *Cell Signal* **19**, 2428-2433 (2007).

42. Nacerddine, K.*, et al.* Akt-mediated phosphorylation of Bmi1 modulates its oncogenic potential, E3 ligase activity, and DNA damage repair activity in mouse prostate cancer. *J Clin Invest* **122**, 1920-1932 (2012).

43. Guzman-Ramirez, N.*, et al.* In vitro propagation and characterization of neoplastic stem/progenitor-like cells from human prostate cancer tissue. *Prostate* **69**, 1683-1693 (2009).

44. Meng, S.*, et al.* Identification and characterization of Bmi-1-responding element within the human p16 promoter. *J Biol Chem* **285**, 33219-33229 (2010).

45. Molofsky, A.V., He, S., Bydon, M., Morrison, S.J. & Pardal, R. Bmi-1 promotes neural stem cell self-renewal and neural development but not mouse growth and survival by repressing the p16Ink4a and p19Arf senescence pathways. *Genes Dev* **19**, 1432-1437 (2005).

46. Rizo, A., Dontje, B., Vellenga, E., de Haan, G. & Schuringa, J.J. Long-term maintenance of human hematopoietic stem/progenitor cells by expression of BMI1. *Blood* **111**, 2621-2630 (2008).

47. Yang, M.H.*, et al.* Bmi1 is essential in Twist1-induced epithelial-mesenchymal transition. *Nat Cell Biol* **12**, 982-992 (2010).

48. Mimeault, M. & Batra, S.K. Frequent gene products and molecular pathways altered in prostate cancer- and metastasis-initiating cells and their progenies and novel promising multitargeted therapies. *Mol Med* **17**, 949-964 (2011).

49. Reya, T., Morrison, S.J., Clarke, M.F. & Weissman, I.L. Stem cells, cancer, and cancer stem cells. *Nature* **414**, 105-111 (2001).

50. Liu, S.*, et al.* Hedgehog signaling and Bmi-1 regulate self-renewal of normal and malignant human mammary stem cells. *Cancer Res* **66**, 6063-6071 (2006).

51. Bisson, I. & Prowse, D.M. WNT signaling regulates self-renewal and differentiation of prostate cancer cells with stem cell characteristics. *Cell Res* **19**, 683-697 (2009).

52. Takebe, N., Harris, P.J., Warren, R.Q. & Ivy, S.P. Targeting cancer stem cells by inhibiting Wnt, Notch, and Hedgehog pathways. *Nat Rev Clin Oncol* **8**, 97-106 (2011).

53. Patrawala, L.*, et al.* Side population is enriched in tumorigenic, stem-like cancer cells, whereas ABCG2+ and ABCG2- cancer cells are similarly tumorigenic. *Cancer Res* **65**, 6207-6219 (2005).

54. Xin, L., Lawson, D.A. & Witte, O.N. The Sca-1 cell surface marker enriches for a prostate-regenerating cell subpopulation that can initiate prostate tumorigenesis. *Proc Natl Acad Sci U S A* **102**, 6942-6947 (2005).

55. White, R.M.*, et al.* Transparent adult zebrafish as a tool for in vivo transplantation analysis. *Cell Stem Cell* **2**, 183-189 (2008).

56. Sabaawy, H.E.*, et al.* TEL-AML1 transgenic zebrafish model of precursor B cell acute lymphoblastic leukemia. *Proc Natl Acad Sci U S A* **103**, 15166-15171 (2006).

57. Stoletov, K., Montel, V., Lester, R.D., Gonias, S.L. & Klemke, R. High-resolution imaging of the dynamic tumor cell vascular interface in transparent zebrafish. *Proc Natl Acad Sci U S A* **104**, 17406-17411 (2007).

Table 1. Primary prostate cancer patient characteristics.

1^{ry} prostate	Age	Type	Grade	pTNM	Gleason
15728	62	Adc	3	pT2c	3 + 3
17148	52	Adc	3	pT2c	3 + 3
17761	57	Adc	3	pT2c	3 + 3
19803	55	Adc	3	pT2c	3 + 3
24126	53	Adc	4	pT3a	3 + 3
40181	60	Adc	4	pT3a	3 + 4
25185	67	Adc	3	pT2c	3 + 3
25315	66	Adc	4	pT3a	3 + 4
26136	67	Adc	3	pT3b	4 + 5
25854	55	Adc	4	pT3b	4 + 5
28838	65	Adc	4	pT3b	4 + 4
28864	68	Adc	3	pT3b	3 + 4
28869	67	Adc	4	pT2c	4 + 4
29032	68	Adc	4	pT3b	4 + 5
29084	58	Adc	3	pT2c	3 + 3
29092	71	Adc	4	pT3b	4 + 4
29110	69	Adc	4	pT3c	4 + 5

Table shows number of each case, age, prostate cancer type (adc, adenocarcinoma), histological grade, pathological staging based on the pTNM classification, where pT2c indicates bilateral prostate disease, and total Gleason scores.

FIGURE LEGENDS

Fig. 1. BMI-1 expression in putative TICs and BMI-1 translational inhibitors. (**a**) The $CD49b^{hi}CD29^{hi}CD44^{hi}$ cells have increased BMI-1 expression. Left, western Blot analysis of BMI-1 expression levels. Right, quantitation of BMI-1 expression levels from 3 independent experiments. Anti-tubulin was used as a loading control. (**b**) Fold adhesion of rapidly adherent $CD49b^{hi}CD29^{hi}CD44^{hi}$ cells [10] with control and BMI-1 knockdown. BMI-1 expression was reduced with sh-BMI-1 lentiviral construct, but not with the non-targeting (sh-Scr) lentiviral control. (**c**) Core chemical structure of BMI-1 small molecule inhibitors. Ar_1 is aryl or heterocyclyl; Ar_2 is heterocyclyl; R^1 is hydrogen; R^2 is hydrogen; and R^3 is C1-8 alkyl. (**d**) Fold adhesion of rapidly adherent $CD49b^{hi}CD29^{hi}CD44^{hi}$ cells treated with BMI-1 inhibitors. (**e**) ELISA assay of BMI-1 levels demonstrating the IC_{50s} of C-209-211 in DU145 cells. (**f**) Western blot analysis of BMI-1 levels in DU145 cells treated with C-209-211 at 1x and 2x of the IC_{50} concentrations. GAPDH levels were used as controls.

Fig. 2. BMI-1 inhibition interferes with self-renewal and spheroid formation *in vitro*. (**a**) Treatment with C-209 reduces the levels of $CD49b^{hi}CD29^{hi}CD44^{hi}$ prostate TICs. DU145 cells were subjected to time-of-adherence assay [10], treated with C-209 for 72 hours, stained, and examined using flow cytometry and Cell Quest software. (**b**) C-209 induces a significant decrease in $CD49b^{hi}CD29^{hi}CD44^{hi}$ TICs phenotype in DU145, PC3 and CWR22 cells. Data are displayed as mean ± SD, and were done in triplicates. (**c**) Effects of BMI-1 inhibitors vs. methotrexate (MTX) and doxorubicin on secondary and tertiary prostate spheroids formation from single cells. Rapidly adherent

$CD49b^{hi}CD29^{hi}CD44^{hi}$ cells were plated on agarose-coated plates. The following day, cells were treated with methotrexate, doxorubicin, C-209 and C-211 at various concentrations for 72 hrs. Post-treatment, primary spheroids were collected, counted and single cell suspensions were plated on 6-well tissue culture dishes for secondary spheroid assays. After 14 days, the formed colonies were stained with crystal violet and counted as secondary spheroids, and displayed on the left as mean ± SD. For tertiary spheroids, single cells from day-7 secondary spheroids were separated, and methotrexate, C-209, and C-211 were added to the spheroids for 72 hrs. Post treatment, tertiary spheroids were stained with crystal violet and counted after 14 days. Data represent three independent experiments using IC_{50} concentrations (*), and 2x IC_{50} concentrations (**), and treatments were found to be statistically significant where indicated (*, **$P<0.005$ compared to untreated).

Fig. 3. Toxicological assays of BMI-1 inhibitors in embryonic zebrafish.

(a) Bright field images of zebrafish embryos treated with BMI-1 inhibitors at the indicated concentrations, and compared to vehicle treatment with DMSO. Progress in normal embryonic development is indicated by hatching of the embryos outside the surrounding chorionic shell at 48-hour post-fertilization (hpf). The dark areas indicate necrotic tissues due to toxic effects. Curling of the tail as in the panels associated with C-211 might represent dorsalization due to interference with embryonic stem cell developmental pathways. (**b**) Survival of zebrafish embryos after 24- and 48-hpf. At least 50 embryos were used in each treatment. Survivals are presented as mean percentage ± SD from three independent experiments. Compounds were dissolved in DMSO and

added to embryo water starting at 12 hpf. (**c**) Western blot analysis demonstrating the effects of C-209 treatment on zebrafish bmi-1a and bmi-1b protein expression. (**d**) Human $CD34^+$ cells grown in methocult for hematopoietic colony assays, and 200 DU145 cells plated in 6-well tissue culture dishes were treated in parallel with C-209 at the indicated concentrations. Colony counts represent three independent experiments ($P<0.0001$ at 1-4 μM).

Fig. 4. Structure, activity, mode of action and antitumorigenic activity of the BMI-1 inhibitor C-209. (**a**) Chemical structure of C-209. (**b**) Antitumor activity of C-209 against DU145 and primary prostate cancer cells. Cells were treated with C-209 at different concentrations for 72hrs. Percentage of survival was calculated using PRIZM software. The IC_{50s} of C-209 against DU145 and primary PCa cells were approximately 2 μM and 1 μM, respectively. (**c**) Treatment with C-209 reduces the levels of $CD49b^{hi}CD29^{hi}CD44^{hi}$ prostate TICs from primary cells. (**d-f**) Primary PCa cell survival, clonogenecity and migration after treatment with DMSO, C-209 or docetaxel. Data are displayed as mean percentage ± SD for cell survival and number of colonies/plate or number of migrated cells from two independent experiments performed with eight distinct patient-derived cells.

Fig. 5. Xenografts of human primary PCa cells in embryonic zebrafish. (**a**) Schematic illustration of the experimental procedure for the use of zebrafish PCa xenografts to identify small molecules targeting BMI-1 *in vivo*. TICs from PCa cells were separated by adherence to collagen, sorted for either high or low expression of

CD49b/CD29/CD44, and then subjected to engraftment in zebrafish embryos and juveniles to demonstrate tumor initiation, and to study the anti-tumor activity of BMI-1 inhibitors *in vivo*. (**b-d**) Histological sections from prostatectomy tissues from prostate cancer patient 24126 stained with H&E. Notice the morphology of the cells in d (arrow). (**e-g**) Formalin fixed paraffin embedded (FFPE) sections from a representative primary PCa tissue used that are stained with dual IHC or single IHC for Erg (in brown) or AMACR (in pink) showing co-expression pattern of both tumor markers (arrows). (**h-k**) Histological sections from a representative zebrafish embryo at 8 dpt demonstrating tumor growth (arrow in i). j-l, Higher magnification of the tumor area in i. Notice that the morphology of the cells in l (arrows) is similar to the primary tissue sample in d. (**l-o**) IHC staining of the section in m showing expression of prostatic specific antigen (PSA) in cells (arrow) of primary PCa fish xenografts. Scale bars are 250 μm in b, e, i, m, and 10 μm in d, f, g, l and p.

Fig. 6. Effects of BMI-1 inhibitor treatment on TICs in zebrafish xenografts. (a) Representative images of vehicle-injected control embryos, and embryos transplanted SC in the tail region with Quantum dots (QD)-labeled primary $CD49b^{hi}CD29^{hi}CD44^{hi}$ cells. Images are overlays of bright field, GFP and red 605 fluorescent images from embryos that developed localized tumors with images taken at 4 days post-transplantation (dpt). (**b**) Anti-tumor activity of C-209. Reduction in tumor size was monitored in outlined area with reduced QD fluorescence (blue arrows). (**c**) Anti-tumor activity of C-209 against xenografts derived from either parental cells (yellow) or the TIC fraction (orange) from the three indicated primary samples. The graph demonstrates responses to C-209 as a

percentage of total xenografts treated (n=25 xenograft per cell fraction per each patient derived cells). Reduction in tumor size is monitored by reduced QD fluorescence. (**d**) Xenografts treated with control (DMSO), C-209 or docetaxel were subjected to IHC for the proliferation marker Ki67. The graph displays percentage ± SD of Ki67+ cells in 100 zebrafish embryo grafted tumor cells. (**e**) Quantitation of tumorigenic capacity of primary PCa TICs in zebrafish xenografts after treatment. Data are displayed as mean percentage ± SD from three independent experiments. (**f**) Diagram showing strategy to study inhibition of tumor initiation potential of primary PCa cell grafts in secondary xenografts. TICs from adherent $CD49b^{hi}CD29^{hi}CD44^{hi}$ cells of three patient samples #40181, #26136, and #25854 were transplanted to generate primary xenografts (1º). Table on the right demonstrates primary graft take rates. Xenograft embryos were treated with either DMSO or C-209 at 2 μM for 72 hours, tumor areas were dissected, pooled, and TICs were sorted and injected into secondary recipients. Treatment with C-209 significantly reduced the rates of secondary xenografts (2º). (**g-h**) IHC of sections of primary and metastatic colonies derived from TICs zebrafish grafts comparing number of cells within each tumor area for BMI-1 expression (arrows). Scale bars are 250 μm in **b** and 50 μm in **g.**

Fig. 7. *In vivo* pharmacological targeting of BMI-1 in mouse PCa xenografts. (**a**) Strategy for examining the antitumor activity of C-209 in serial mouse xenografts and clonogenic repopulation assays of xenograft cells treated with C-209. (**b**) C-209 effectively inhibited BMI-1 production in tumor tissues *in vivo*. PCa cells were implanted SC in NSG mice and, after tumor development, mice were randomized and administered

C-209 SC at a dose of 60 mg/kg/day for ten days. Treatment with C-209 significantly inhibited tumor growth (n=8 mice /group, ***p<0.002). (**c**) Images are H&E staining of mouse xenograft sections indicating the histological effects of treatments. (**d**) Intratumor IHC revealed reduced nuclear BMI-1 (brown) and surface CD44 (red) staining (400X total magnification) upon treatment with C-209. Areas that were less necrotic in the peripheral tumor part away from the center of the xenograft tumor were selected for imaging. Treatment with C-209 was associated with a significant intratumor reduction in Ki67 positive cells. Ki67 images are shown with 50X and 100X magnification. (**e**) Quantitation of Ki67 positive cells in sections from treated xenografts. (***p<0.002). (**f**) Clonogenic abilities of cells dissociated from treated tumors in mice according to the diagram in **a** in self-renewal assays. (*p<0.01, ***p<0.001) (**g**) Tumor initiation potential in serial grafting in secondary mouse xenografts of cells dissociated from treated primary mouse xenografts (n=8 mice /group).

Fig. 1

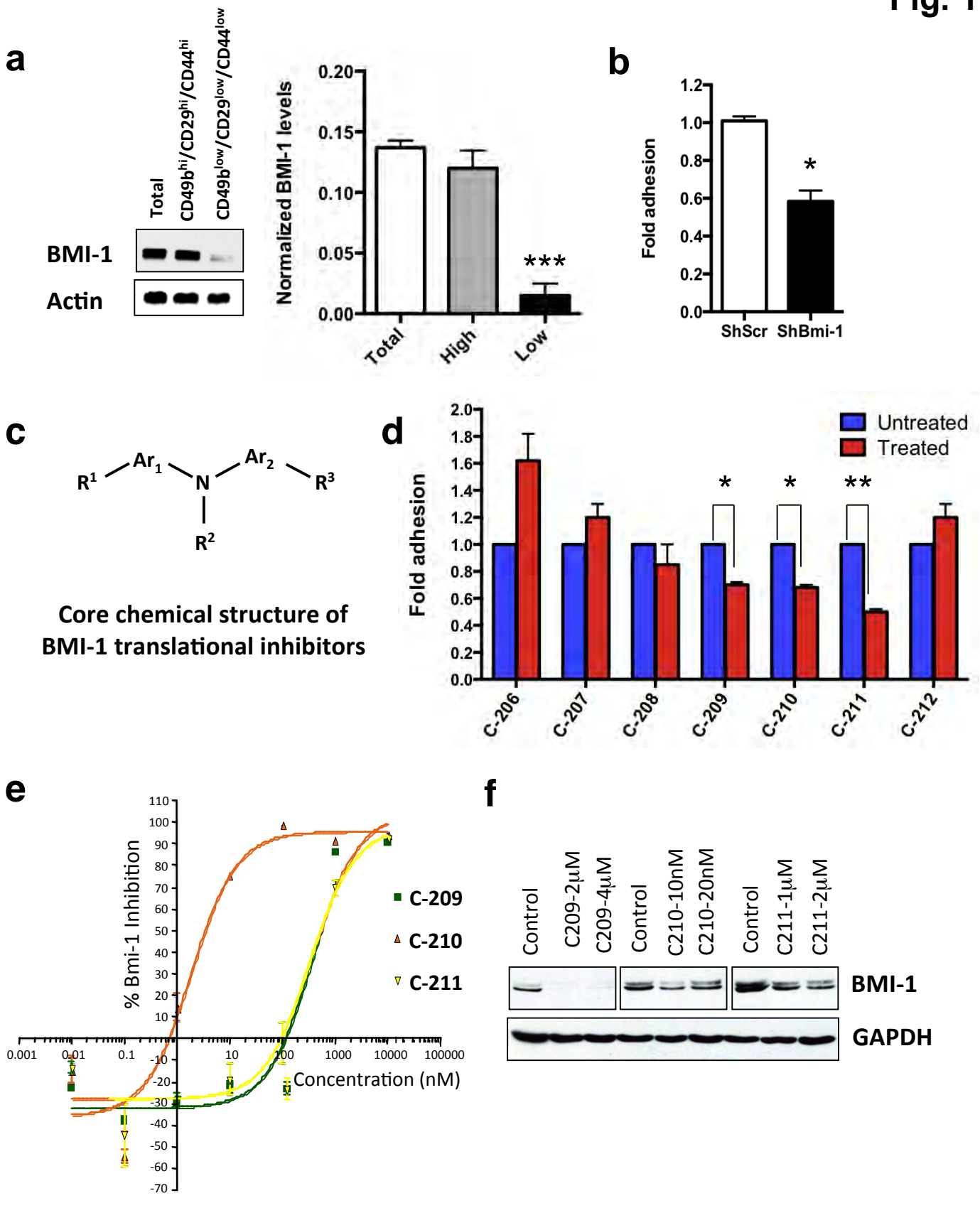
a
Total
CD49b^hi/CD29^hi/CD44^hi
CD49b^low/CD29^low/CD44^low
BMI-1
Actin
Normalized BMI-1 levels
0.20
0.15
0.10
0.05
0.00
***
Total
High
Low
b
Fold adhesion
1.2
1.0
0.8
0.6
0.4
0.2
0.0
*
ShScr
ShBmi-1
c
R1
Ar1
N
Ar2
R3
R2
Core chemical structure of
BMI-1 translational inhibitors
d
Fold adhesion
Untreated
Treated
2.0
1.8
1.6
1.4
1.2
1.0
0.8
0.6
0.4
0.2
0.0
*
*
**
C-206
C-207
C-208
C-209
C-210
C-211
C-212
e
% Bmi-1 Inhibition
110
100
90
80
70
60
50
40
30
20
10
-10
-20
-30
-40
-50
-60
-70
0.001
0.01
0.1
10
100
1000
10000
100000
Concentration (nM)
C-209
C-210
C-211
f
Control
C209-2μM
C209-4μM
Control
C210-10nM
C210-20nM
Control
C211-1μM
C211-2μM
BMI-1
GAPDH

Fig. 2

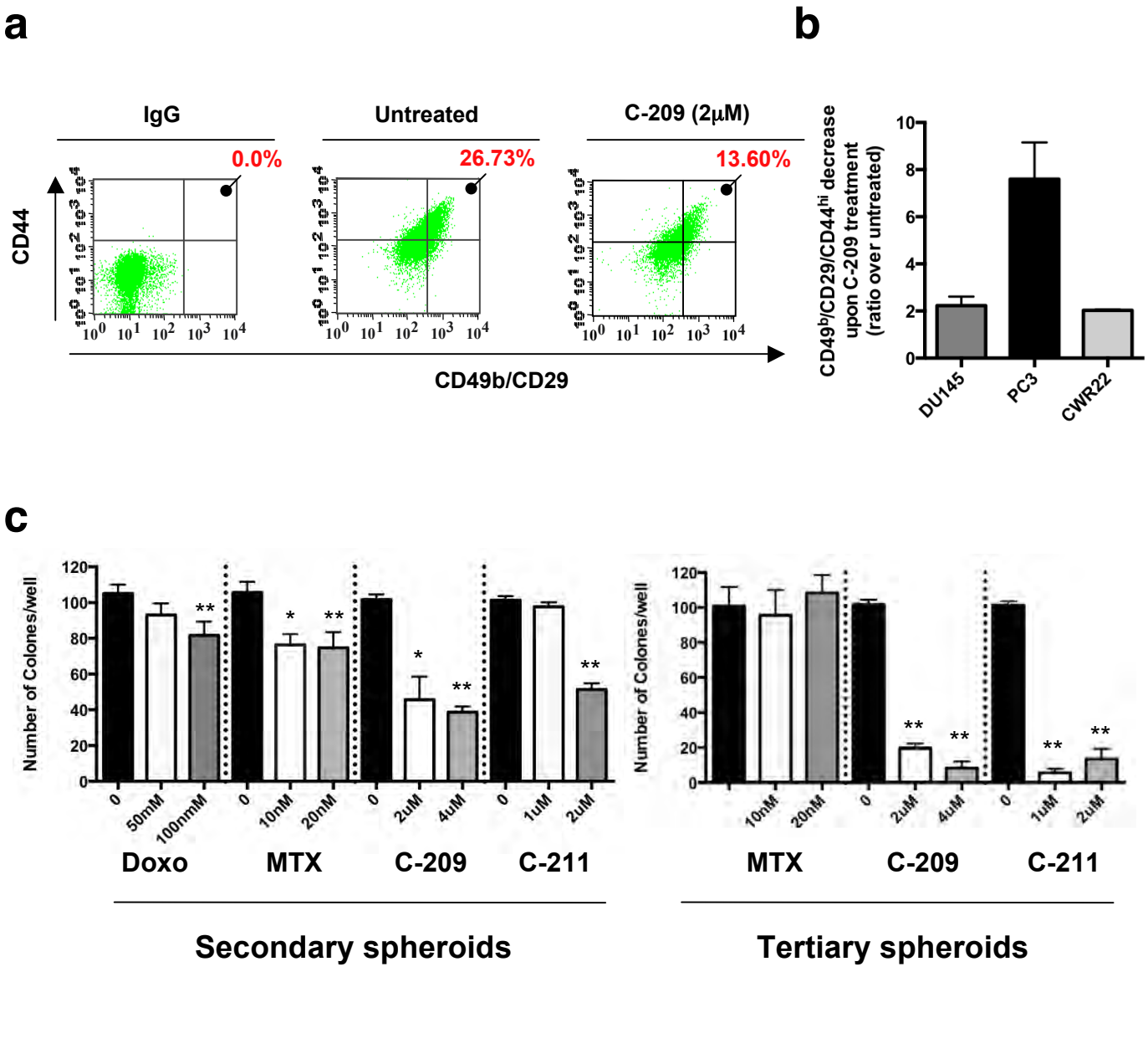
a
IgG
Untreated
C-209 (2μM)
0.0%
26.73%
13.60%
CD44
CD49b/CD29
b
CD49b/CD29/CD44hi decrease upon C-209 treatment (ratio over untreated)
DU145
PC3
CWR22
c
Number of Colones/well
0
50mM
100mM
10nM
20nM
2uM
4uM
1uM
Doxo
MTX
C-209
C-211
Secondary spheroids
Tertiary spheroids

Fig.3

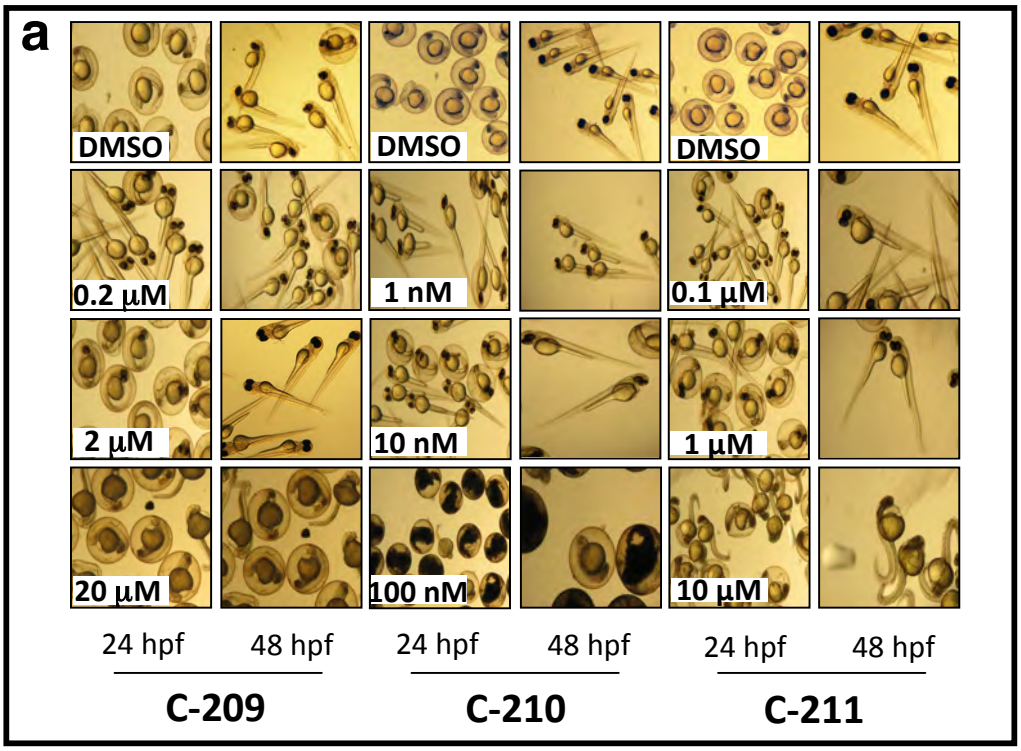

b **Survival of zebrafish embryos after treatment with BMI-1 inhibitors (%)**

	DMSO	C-209 (μM)			C-210 (nM)			C-211 (μM)		
		0.2	2	20	1	10	100	0.1	1	10
24 hpf	98 ± 1	97 ± 1	98 ± 1	90 ± 3	98 ± 1	96 ± 4	0	99 ± 1	98 ± 1	0
48 hpf	98 ± 1	98 ± 1	97 ± 2	65 ± 4	97 ± 1	90 ± 4	0	98 ± 1	98 ± 1	0

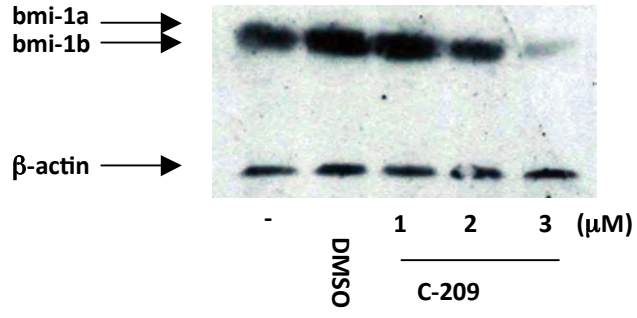

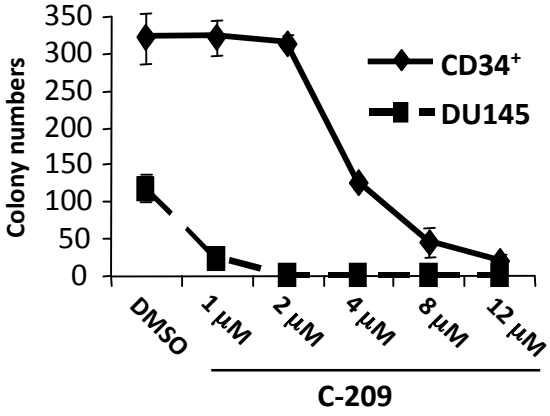

Fig. 4

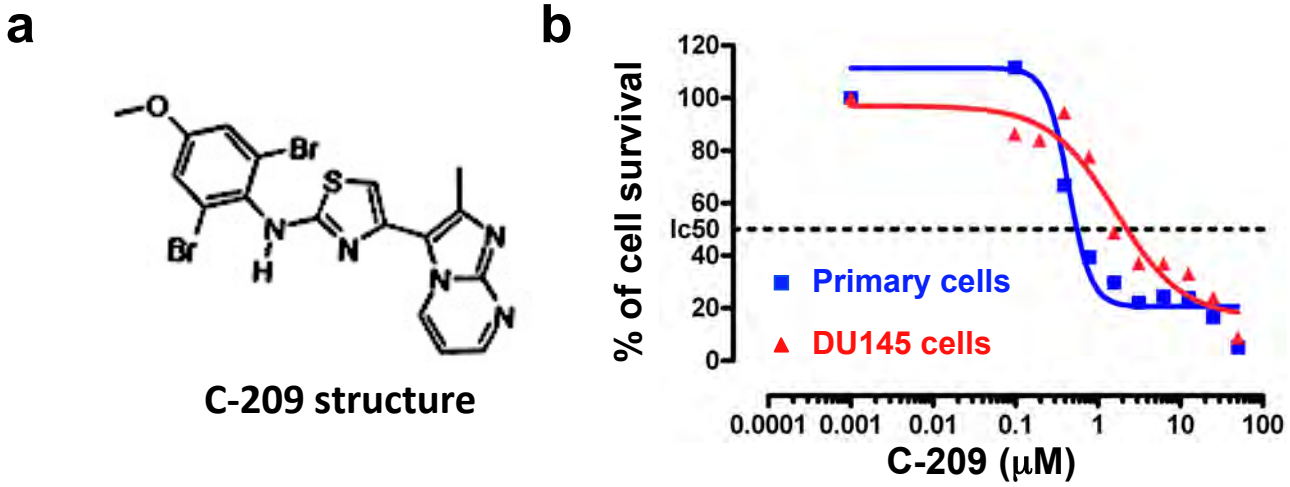
a
b
C-209 structure
% of cell survival
Ic50
Primary cells
DU145 cells
C-209 (μM)

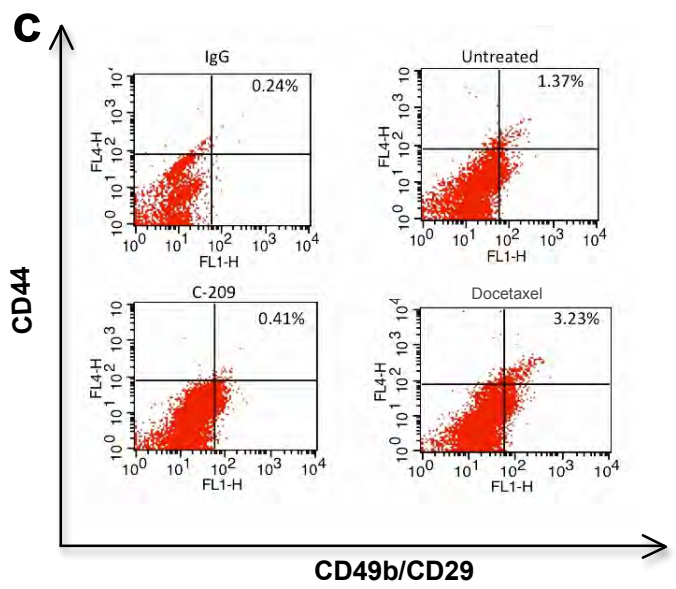
c
IgG
0.24%
Untreated
1.37%
C-209
0.41%
Docetaxel
3.23%
CD44
CD49b/CD29

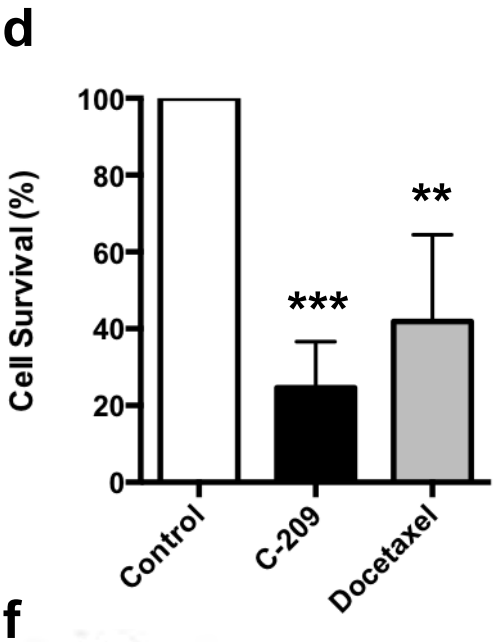
d
Cell Survival (%)
Control
C-209
Docetaxel

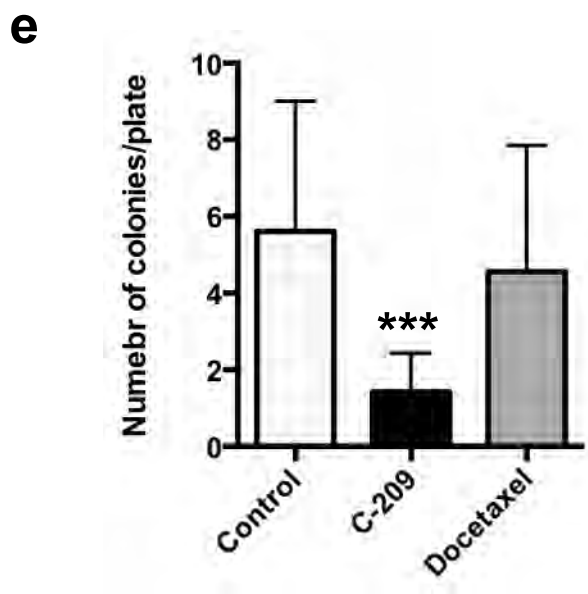
e
Numebr of colonies/plate
Control
C-209
Docetaxel

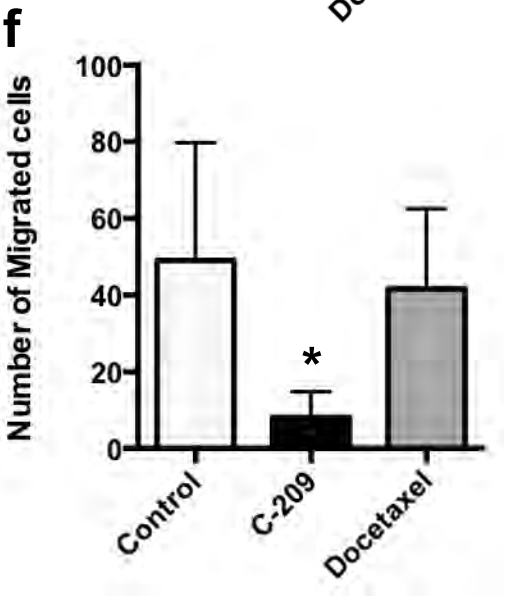
f
Number of Migrated cells
Control
C-209
Docetaxel

Fig. 5

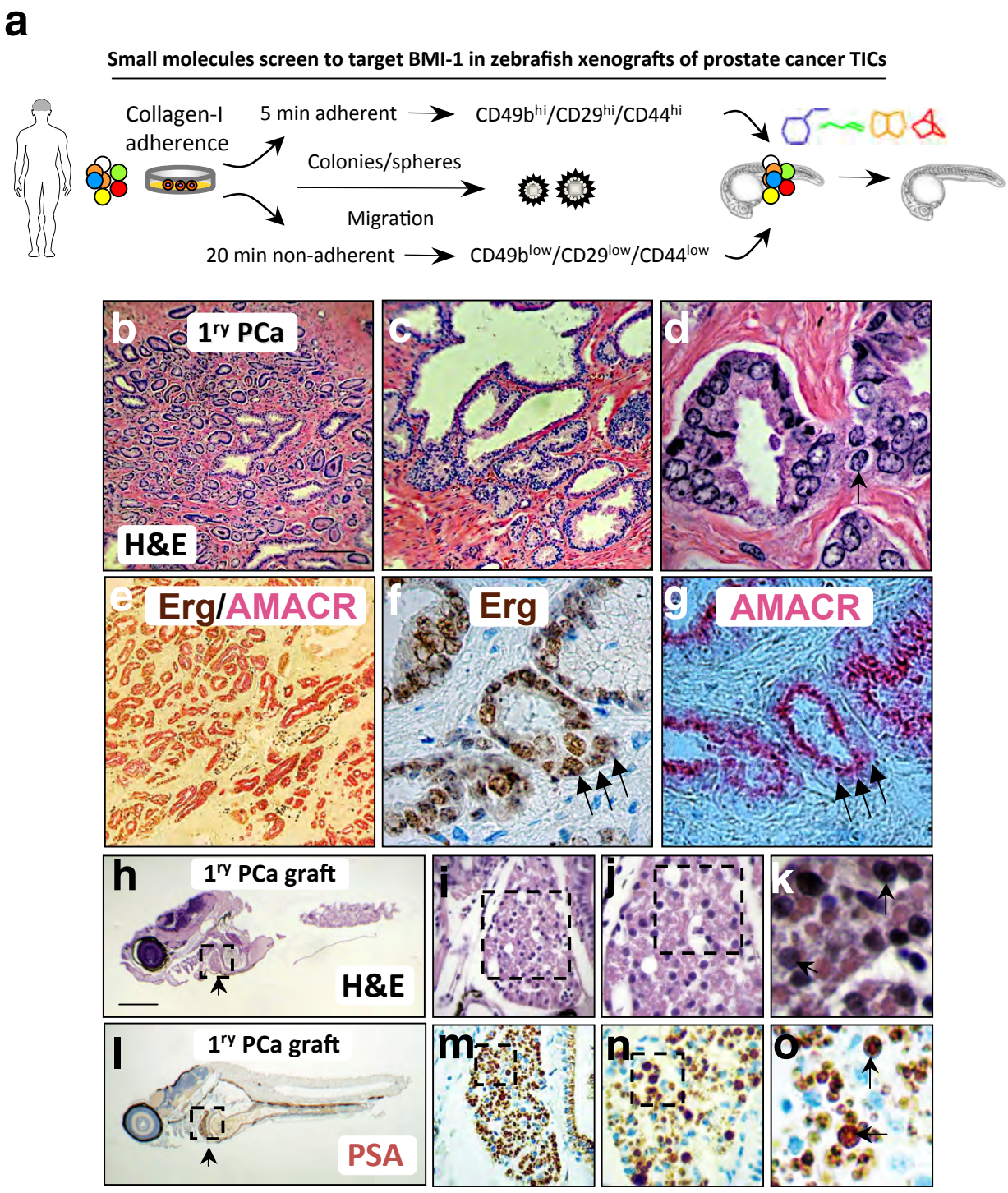
a
Small molecules screen to target BMI-1 in zebrafish xenografts of prostate cancer TICs
Collagen-I adherence
5 min adherent
CD49b^hi/CD29^hi/CD44^hi
Colonies/spheres
Migration
20 min non-adherent
CD49b^low/CD29^low/CD44^low
b
1ry PCa
H&E
c
d
e
Erg/AMACR
f
Erg
g
AMACR
h
1ry PCa graft
H&E
i
j
k
l
1ry PCa graft
PSA
m
n
o

Fig. 6

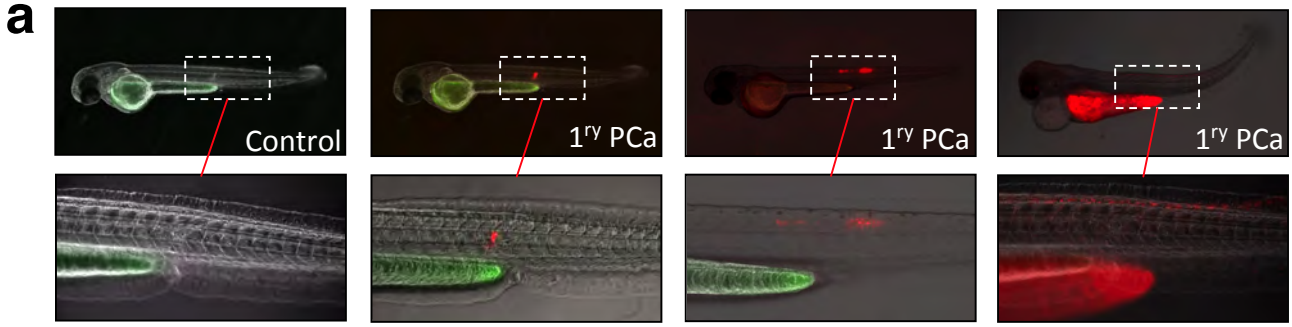

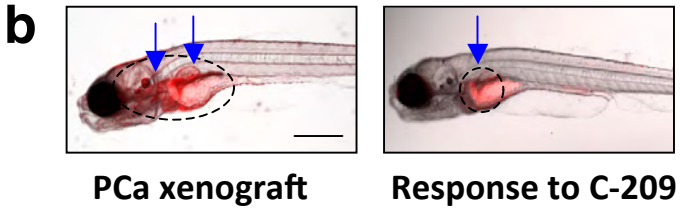

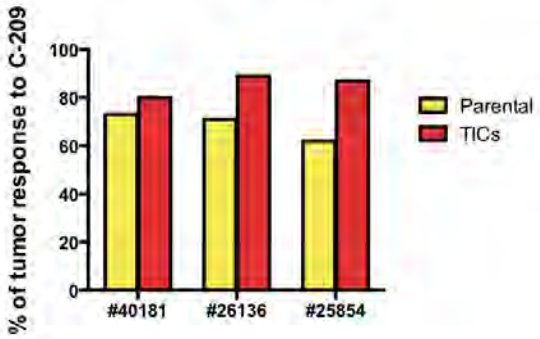

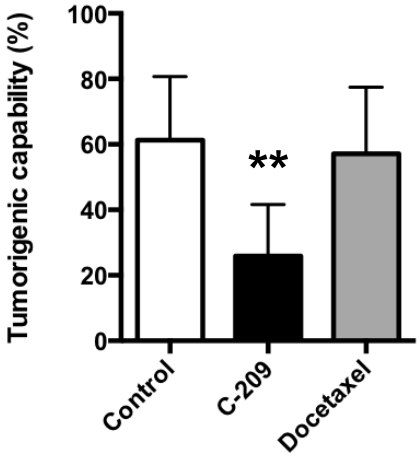

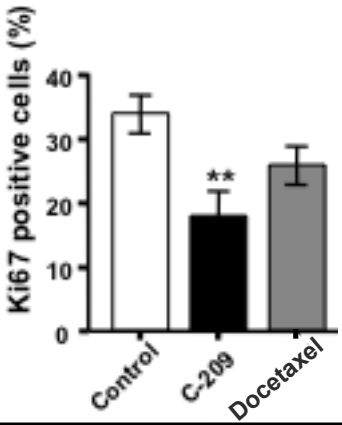

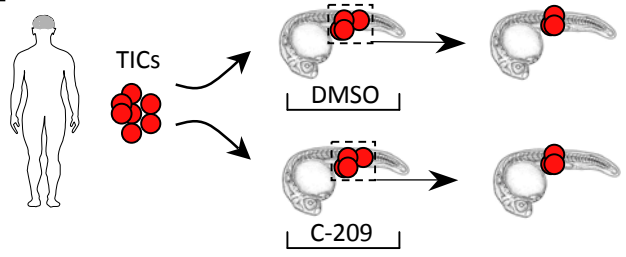

1º tumor	1º graft take n(%)	Rx	2º graft take n(%)
40181	21/25 (84)	DMSO	18/23 (78)
	25/32 (78)	C-209	4/28 (14)*
26136	14/16 (87)	DMSO	14/18 (78)
	10/15 (67)	C-209	8/25 (32)*
25854	18/23 (78)	DMSO	22/25 (88)
	15/18 (83)	C-209	10/22 (45)*

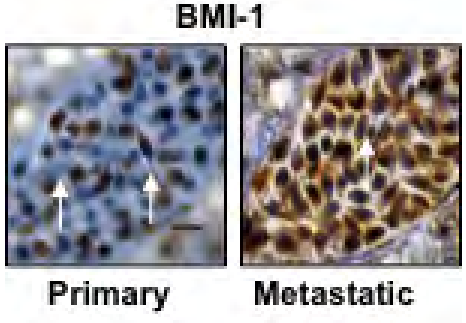

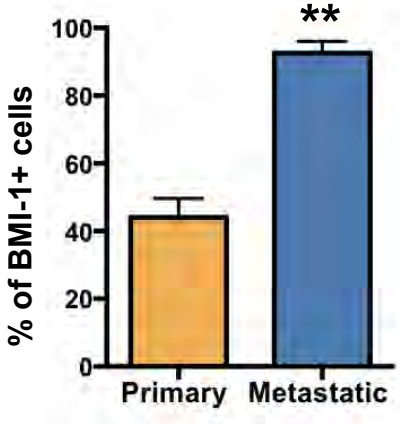

Fig. 7

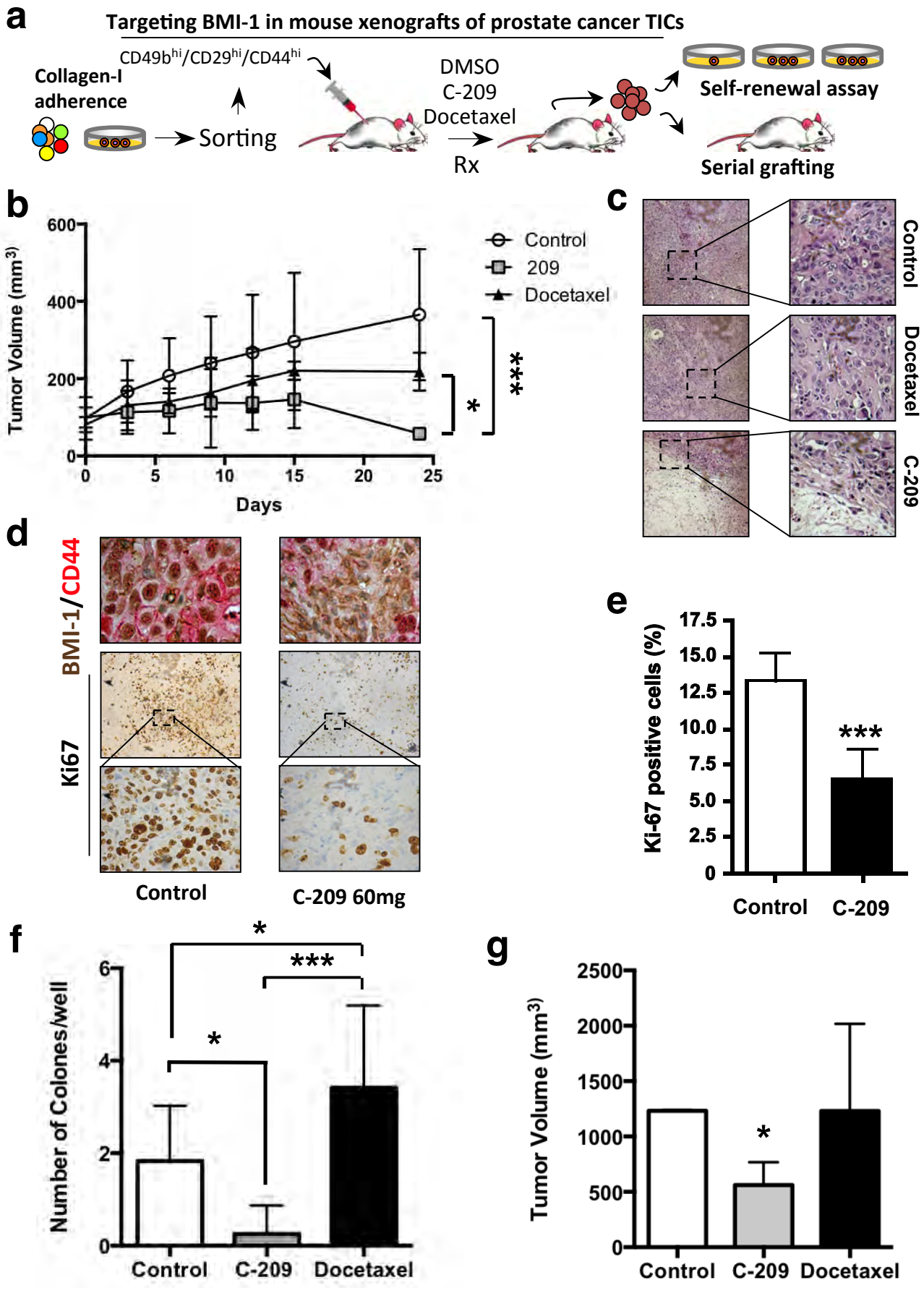
a
Targeting BMI-1 in mouse xenografts of prostate cancer TICs
CD49b^hi/CD29^hi/CD44^hi
Collagen-I adherence
Sorting
DMSO
C-209
Docetaxel
Rx
Self-renewal assay
Serial grafting
b
Tumor Volume (mm3)
Days
Control
209
Docetaxel
*
***
c
Control
Docetaxel
C-209
d
BMI-1/CD44
Ki67
Control
C-209 60mg
e
Ki-67 positive cells (%)
***
Control
C-209
f
Number of Colones/well
*
***
*
Control
C-209
Docetaxel
g
Tumor Volume (mm3)
*
Control
C-209
Docetaxel

SUPPLEMENTARY DATA

Selective BMI-1 targeting interferes with tumor-initiating cell survival and tumor growth in prostate cancer

Nitu Bansal, Monica Bartucci, Shamila Yusuff, Stephani Davis, Kathleen Flaherty, Eric Huselid, Liangxian Cao, Nadiya Sydorenko, Young-Choon Moon, Hua Zhong, Daniel J. Medina, Mark N. Stein, Isaac Y. Kim, Thomas W. Davis, Robert S. DiPaola, Joseph R. Bertino, Hatem E. Sabaawy

SUPPLEMENTARY FIGURES

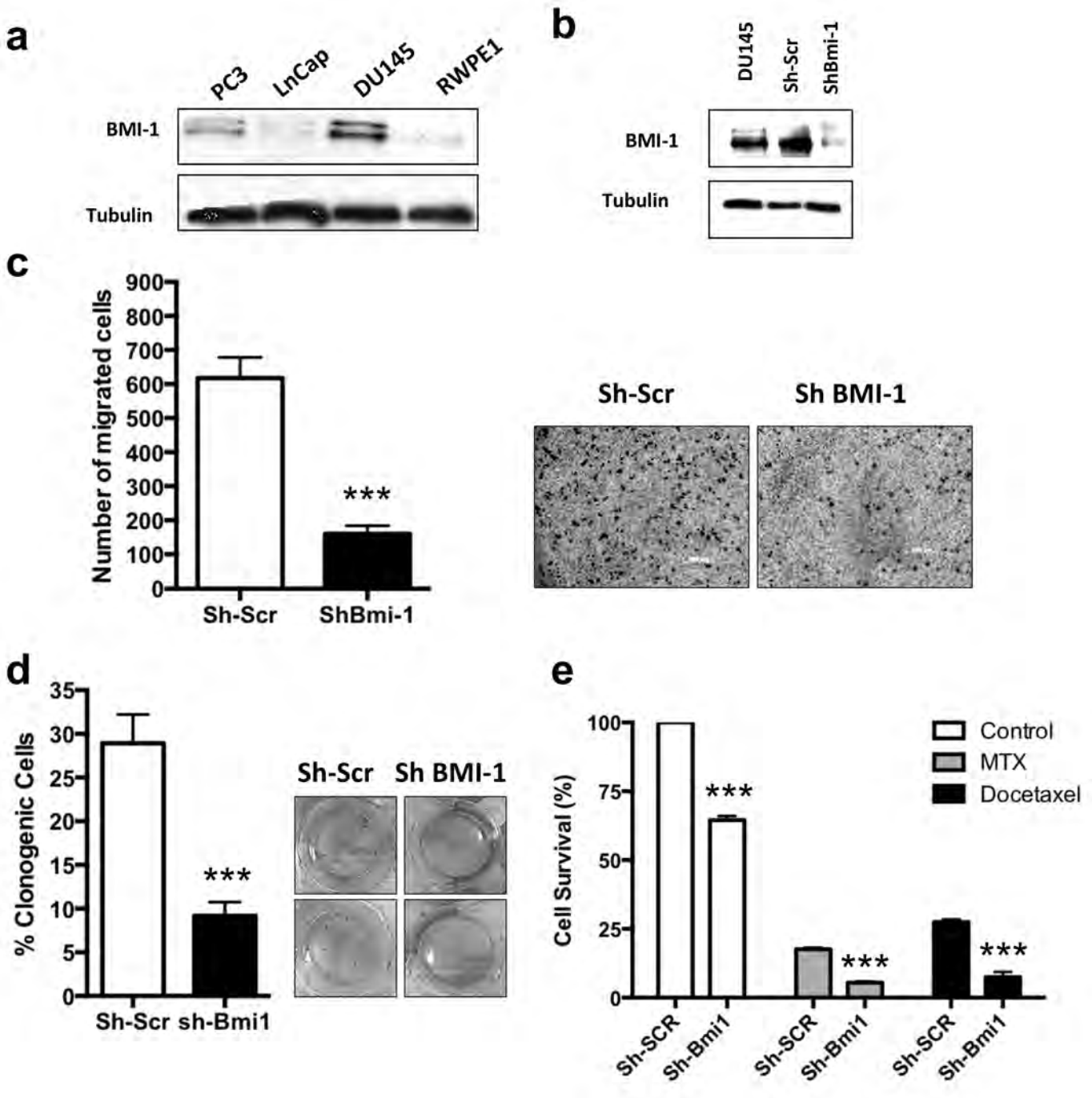

Supplementary Fig. 1. Functional role(s) of BMI-1 in PCa. (**a**) Western Blot analysis for BMI-1 expression in prostate cancer cell lines (PC3, LNCap, and DU145), and in immortalized normal prostate epithelial cells (RWPE-1). (**b**) BMI-1 expression is reduced with sh-BMI-1 lentiviral construct, but not with the non-targeting scrambled (sh-Scr) lentiviral control. Representative western blot and images from three independent experiments (***$p<0.001$). (**c**) Right: Illustrative pictures of Sh-Scramble and Sh-Bmi-1 infected cells migration capacity. Cell motility was assessed after 24 h incubation in modified boyden chambers (Scale bars 200μm). Left: Graph showing the number of migrated cells in standard growth conditions. Data are showing the outcome of three independent experiments. (**d**) Percentage of clonogenic cells upon BMI-1 knockdown compared to sh-Scr lentiviral control (**$p<0.01$). Images on the right demonstrate colonies derived from infected cells and stained with crystal violet. (**e**) Percentage of cell survival upon combined knockdown of BMI-1 and treatment with chemotherapeutic agents methotrexate (MTX) or taxotere (TXT) compared to DMSO controls (***$p<0.001$).

a

Drugs	IC_{50}
Doxorubicin	50 nM
Docetaxel	2.5 nM
Methotrexate	10 nM
C-206	1.5 μM
C-207	1 μM
C-208	1 μM
C-209	2 μM
C-210	10 nM
C-211	1 μM
C-212	10 nM

b

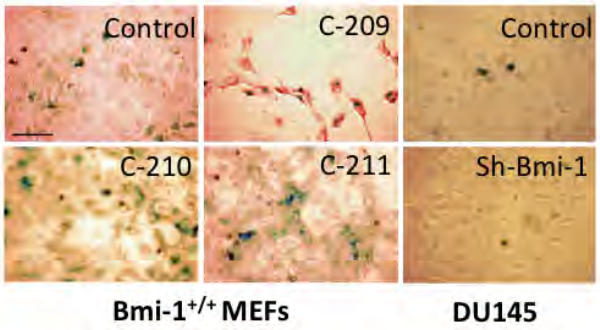

c

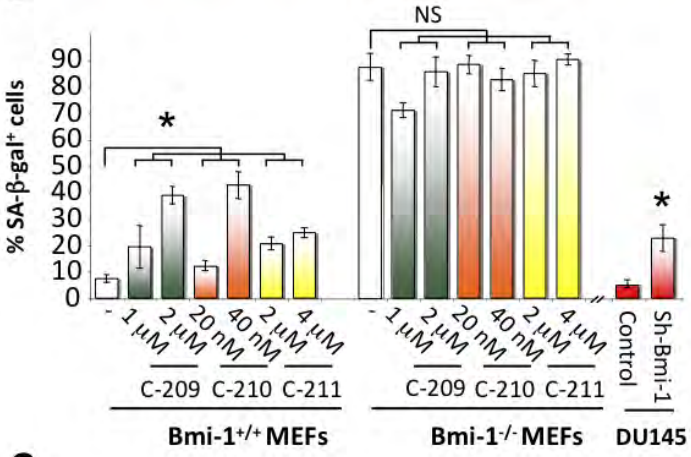

d

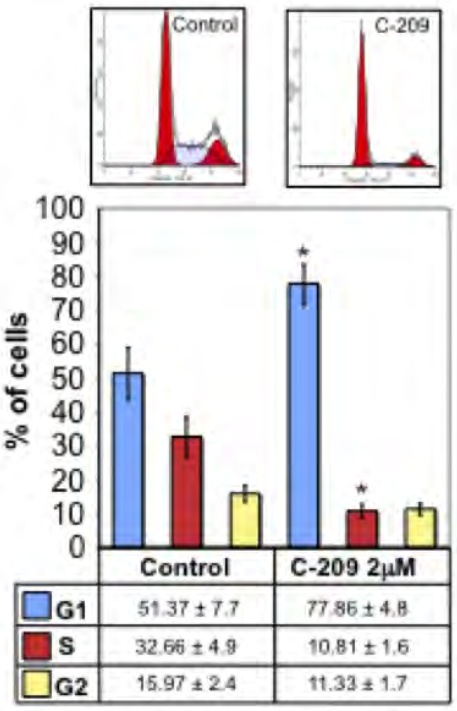

	Control	C-209 2μM
G1	51.37 ± 7.7	77.86 ± 4.8
S	32.66 ± 4.9	10.81 ± 1.6
G2	15.97 ± 2.4	11.33 ± 1.7

e

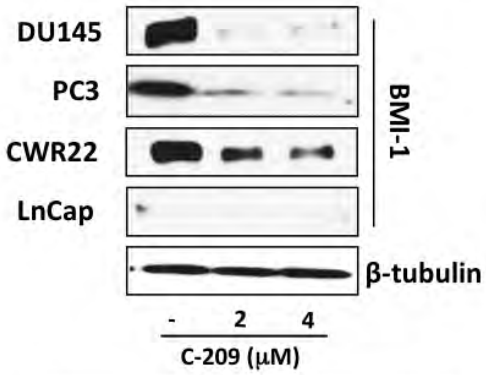

f

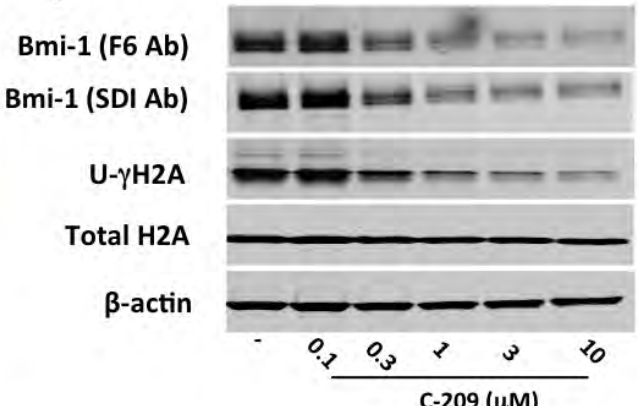

Supplementary Fig. 2. Pharmacological inhibition of BMI-1. (**a**) IC_{50} concentrations of doxorubicine, methotrexate, docetaxel and Bmi-1 inhibitors C-206 to C-212. IC_{50}s were determined using MTS assays in DU145 cells. (**b**) SA-β-gal staining of mouse embryonic fibroblasts (MEFs) and DU145 cells treated with C-209, C-210, or C-211. The reduced cell density in the image after treatment with C-209 is due to significant killing of DU145 cells. Scale bar is 50 μm. (**c**) Quantitation of SA-β-gal staining in control and C-209-, C-210-, or C-211-treated MEFS with (Bmi-$1^{+/+}$) or without Bmi-1 expression (Bmi-$1^{-/-}$), and in sh-Bmi-1 targeted DU145 cells. Note that Bmi-1-null MEFs have high levels of senescence. (*$p<0.01$ compared to untreated cells, NS, not significant). (**d**) Cell cycle analyses of DU145 cells treated with C-209. Top images and mean ± SD are representative of three analyses. G1 cell cycle arrest was associated with a significant reduction in the percentage of cells in S phase. (**e**) BMI-1 expression levels in DU145, PC3, CWR22 and LnCap PCa cells treated with increasing concentrations of C-209. β-tubulin (shown only from DU145 cells) was used as loading control. (**f**) Cells treated with C-209 were investigated for the expression of BMI-1 using two different antibodies (Targeting the carboxyl terminal or the full-length protein). Notice the dose-dependent reduction of the C-terminal lysine-119 mono-ubiquitinated form of γ-H2A (U), a specific product of the BMI-1/PRC1 complex, compared to total H2A and β-actin.

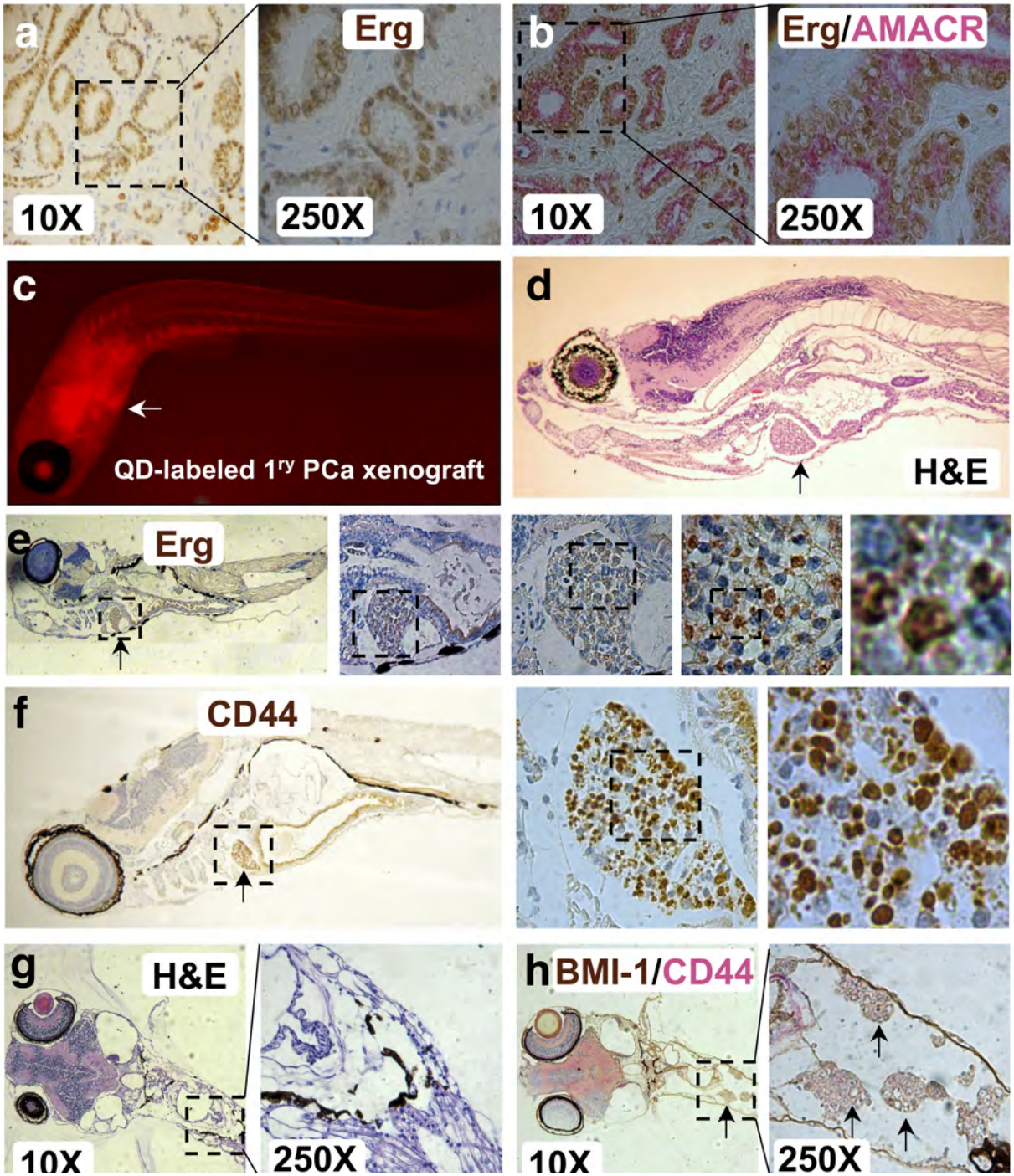

Supplementary Fig. 3. Xenografts of primary PCa tissue in zebrafish embryos. (**a**) Section from primary PCa tissue identified to harbor the TEMPRESS-Erg fusion by FISH (not shown) demonstrates overexpression of Erg (brown) by IHC. (**b**) Co-localization of Erg (brown) and AMACR (pink) in PCa glands demonstrated by dual IHC staining. (**c**) Representative embryos transplanted with quantum-dot (QD) labeled primary PCa cells showing tumor formation as measured by red fluorescence at the 605 QD filter. (**d**) Histological sections from a representative zebrafish embryo at 8 days post-transplantation (dpt) of the mirrorimages of primary cells in a

demonstrating expression of Erg in the tumor graft cells (arrow in with higher magnifications in the right panels). (**f**) A representative zebrafish embryo at 12 dpt of the mirrorimages of primary cells in a demonstrating expression of CD44 in the tumor graft cells (arrow in with higher magnifications in the right panels). (**g-h**) Co-expression of CD44 and BMI-1 in the tumor graft cells (outlined areas in g and arrows in h). Scale bars are 250 μm in a-b, d, f, and 100 μm in e and g-h.

Supplementary Fig. 4. Toxicology assays of chemotherapy and BMI-1 inhibitors in embryonic zebrafish. Bright field images of zebrafish embryos treated with chemotherapy and BMI-1 inhibitors at IC_{50} concentrations, and compared to vehicle treatment with DMSO. In these conditions, compounds were added to embryo water after 6 hours post-fertilization (hpf) to examine the effects of these compounds on embryos that will be harboring tumor xenografts upon transplantation at 48-72 hpf and establish background fluorescence for treated embryos in the absence of human tumor cells. Treatment compounds when used at IC_{50} concentrations had no notable toxic effects. At least 20 embryos were used in each treatment. Taxol, docetaxel; MTX, methotrexate.

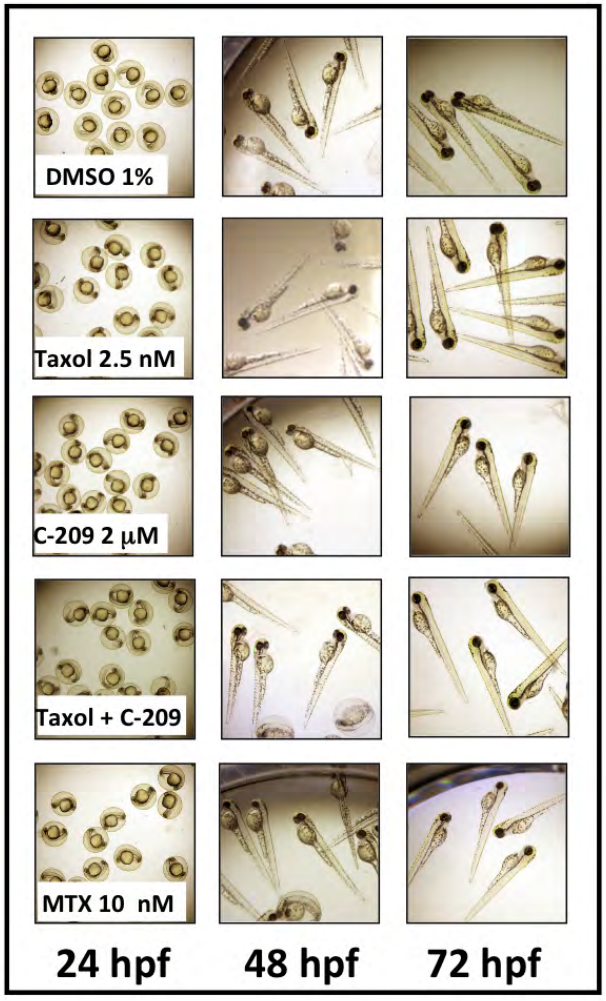

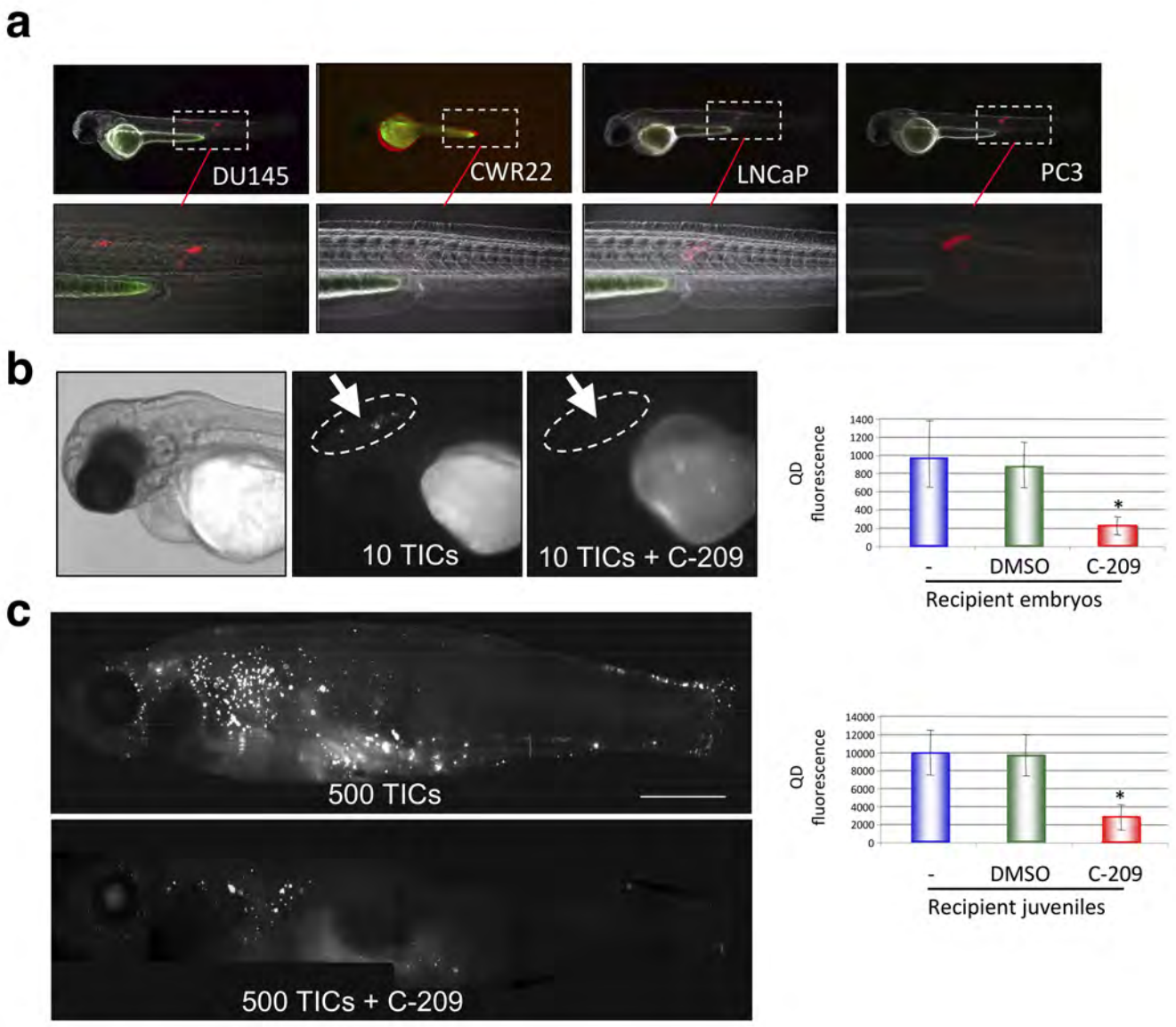

Supplementary Fig. 5. Anti-tumor activity of BMI-1 inhibitors. (**a**) Representative images of embryos transplanted SC in the tail region with Q-dots-labeled rapidly adherent CD49b^{hi}CD29^{hi}CD44^{hi} (TICs) CWR22, LNCap, PC3, DU145 cells. Non-tumorigenic normal prostate cells were used as control and yielded no tumor formation. Images are overlays of bright field, GFP and red 605 fluorescent images from embryos that developed localized tumors with images taken during tumor development at 4 dpt. (**b**) Transplantation of 10 TICs resulted in brain metastasis in zebrafish embryos (arrow in outlined area). Exposure of the same embryo to the BMI-1 inhibitor C-209 at 2 μM in the water for 72 hours reduces the size and fluorescence emitted by DU145 cells growing in zebrafish embryonic brain (compare circled areas before and after treatment). Bright field image of this treated embryo is corresponding to the fluorescent image after treatment. Right graph demonstrates the QD fluorescence emitted by the tumor masses in outlined tumor regions of either untreated,

vehicle, or C-209 treated embryos that were measured and displayed in arbitrary fluorescence units reflecting tumor growth or regression after treatment for 72 hours. Data are representatives from 8 independent experiments displayed as mean ± SD derived from three replicate experiments using ≥20 embryo/group (*p<0.001). (**c**) Florescent composite images of whole juvenile zebrafish recipients of DU145 TICs transplant. Images are lateral views with the head to the left. Transplant of 500 TICs in conditioned juvenile zebrafish resulted in tumor growth, widespread migration, and metastasis of QD-labeled tumor cells throughout the fish. Exposure to the BMI-1 inhibitor C-209 at 2 μM in the water for 5 days reduced the size and fluorescence emitted by DU145 cells. The graph demonstrates QD fluorescence emitted by tumor masses in juvenile fish that are either untreated, vehicle, or C-209 treated and were measured, and displayed in arbitrary fluorescence units reflecting tumor growth or regression. Data are displayed as mean ± SD derived from three experiments using 3 juvenile fish/group (*p<0.001).

SUPPLEMENTARY METHODS

Western blot analyses

Pelleted cells were lysed and total proteins at 70-100 μg were separated on SDS PAGE gels, and were analyzed using mouse monoclonal anti-Bmi-1 clone F6 against the N-terminal (1:1000) (Millipore), rabbit polyclonal anti-Bmi-1 SDI against the C-terminal (1:2,000) (SDI), mouse monoclonal anti-ubiquityl (γ)-histone H2A clone E6C5 (1:1,000) (Millipore), rabbit polyclonal anti-H2A (total) (1:1,000) (Millipore), and anti-tubulin (1:100) (Abcam).

shRNA-mediated knockdown of Bmi-1

For knockdown, DU145 cells were transfected with GIPZ Bmi-1 shRNA construct (Open Biosystems) using lipofectamine. Bmi-1 shRNA positive cells were selected in media with 0.5 μg/ml of puromycin. Cell growth was monitored and collagen-I attachment assays were done once sufficient cells were obtained.

Selection was carried out by exposition to puromycine 5 μg/ml (Sigma).

Cell viability assays

For cell viability studies, 5 $x10^3$cells/well were plated in 96-well plates. Docetaxel (2.5nM) or metotrexate (10nM) were used to evaluate sensitivity to chemotherapy. Cell viability was evaluated after 48hrs through MTT assay.

Migration assay

Cell migration was assessed in 24-well transwell boyden chambers (Costar Scientific Corporation, Cambridge, MA). Single cells ($2x10^4$) were suspended in a complete growth medium and placed into upper chambers. After incubation for 24 hrs, migrated cells were stained with Coomassie Brilliant Blue and counted.

Soft agar colony forming assays

To evaluate the fraction of self renewing cells, 500 cells were plated in the top agar layer in each well of a 24-well culture plate with 0.3% top agar layer and 0.4% bottom agar layer (SeaPlaque Agarose, Cambrex, NJ). Cultures were incubated at 37°C for 20 days. Colonies were stained after 3 weeks with crystal violet (0.01% in 10% MetOH), visualized and counted under microscope and photographed.

Immunohistochemistry (IHC) and BMI-1 knockdown

For IHC, fixed paraffin-embedded tissue samples from normal human prostate, prostate tumors, and xenografts were stained with anti-BMI-1 or other antibodies using antigen retrieval methods, and sections were scored for percentage of cells as well as intensity on a 0-2 scale by pathologists blinded to treatment.

β-gal assay for senescence

Senescence experiments were performed in two 6-well plates for each treatment. Percentage of senescent cells was determined based on counts of 1,000 cells per treatment. Treatment with C-209 resulted in significant increase in senescence of DU145 cells that was detected with β-gal staining. Cells were fixed in 4% paraformaldehyde, washed in PBS pH 7.4 followed by PBS pH 6.0 for one hour each. Fixed cells were then stained with 2μg/ml x-gal (Sigma) overnight at 37°C and washed with PBS pH 6.0. Cells were imaged and staining was quantitated using Adobe Photoshop and ImageJ. The β-gal staining intensity was measured using the average intensity density of hue saturation.

Cytotoxicity assays

Cytotoxicity of C-209, C-210, and C-211 compounds (PTC therapeutics) and methotrexate, doxorubicin and docetaxel were assayed following a 3-day exposure. DU145 Cells (3×10^3 cells/well) were treated with multiple concentrations to determine an IC_{50}, and cytotoxicity was analyzed using MTS assay (Sigma) per manufacturer's instructions. IC_{50} concentrations were determined using Hill's equation in Graph-Pad prism 4.0 software.

Transplantation of human prostate cancer cells in zebrafish

Cells were resuspended in 0.5x Dulbecco's PBS (DPBS) containing QD605 (red fluorescence) (QD605; Invitrogen) and lipofectamine at a ratio of 1:2 for 2 hours. Cells were suspended in 0.5x DPBS for transplantation into dechorionated and anesthetized (0.5x tricaine methanesulfonate, MS-222; Sigma) 48-hour post fertilization (hpf) embryos using 15 μm (internal diameter) injection needles. Injections were either subcutaneously (SC), or above the yolk into the sinus venosus using a Celltram microinjector. After transplantation, embryos were incubated for 2 hours at 37°C, and were then maintained in a humidified incubator at 33°C. Human cells were monitored under fluorescent microscopy for homing and tissue repopulation.

Subject: Decision on manuscript NCOMMS-14-10824
Date: Monday, September 8, 2014 8:14:14 PM ET
From: Tanya.Bondar@us.nature.com
To: Sabaawy, Hatem

** Please ensure you delete the link to your author home page in this e-mail if you wish to forward it to your coauthors **

Dear Prof Sabaawy,

Your manuscript entitled "Selective BMI-1 targeting interferes with tumor-initiating cell survival and tumor growth in prostate cancer" has now been seen by 4 referees, whose comments are appended below. While they find your work of potential interest, they have raised substantive concerns that in our view preclude publication of the manuscript in Nature Communications, at least in its present form.

Should further experimental data allow you to address these criticisms, including but not limited to the selectivity of the inhibitor towards Bmi1 and its specific mode of action, we would be quite happy to look at a revised manuscript (unless something similar has been accepted at Nature Communications or appeared elsewhere in the meantime). However I should stress that, because Nature Communications strives to provide an efficient editorial service and fast publication, we are reluctant to see manuscripts undergo multiple rounds of review and would be unlikely to offer you more than one more chance to satisfy our reviewers. In the case of eventual publication, the received date would be that of the revised paper.

In the event of resubmission, please use the following link to submit your revised manuscript and a point-by-point response to the referees:
http://mts-ncomms.nature.com/cgi-bin/main.plex?el=A7S2QCQ2A4ETHK4I6A9ftd2NKFbcAnUDDe94D0SrcWwZ

** This url links to your confidential home page and associated information about manuscripts you may have submitted or be reviewing for us. If you wish to forward this email to co-authors, please delete the link to your homepage first **

In the meantime, we hope you will find our referees' comments helpful in deciding how to proceed. Please do not hesitate to contact us if there is anything you would like to discuss.

Best regards,

Tanya Bondar PhD
Assistant Editor
Nature Communications

Reviewers' comments:

Reviewer #1 (Remarks to the Author):

In this manuscript Bansal et al identified small molecules that target Bmi-1 expression. They showed by various in vivo and in vitro assays that treatment with the compounds can suppress tumor growth and reduce the TIC percentage. They suggest that Bmi-1 can serve as a target for prostate cancer treatment. The strategy to identify the putative Bmi-1 inhibitor is impressing and the application of the zebrafish xenograft model is interesting. However, a few major issues that serve as the basis of this study have not been clearly addressed, which weaken the conclusion

of the study and dampen the enthusiasm towards it.
(1) How is the specificity of this compound and how does it work? The authors did not present extensive studies addressing these questions. They showed using in vitro senescence assay that the compound can cause senescence. However, this does not address the question of specificity. It is not known how the compound works. How soon the expression of Bmi-1 is affected? Does it affect transcription or translation? What is the overall transcriptional profile looks like in cells before and after compound treatment. How do Bmi-1 null or low cells respond to the drug in various aspects of cell biology other than senescence? Without a clear understanding of how the compound works, the impact of the study is questionable.
(2) On page 9, the authors claimed that the compound does not affect normal stem cells and used the hematopoietic stem cells as an example. However, the data were not shown. It is not clear how the compound affects the expression of Bmi-1 in HSC. How does this concur with previous study showing Bmi-1 being essential for the maintenance of HSC? The conclusion from this section is not supported by extensive analysis in whole mouse body and is not convincing.
(3) In Fig 7g, in order to demonstrate that TIC cells are affected, the authors need to do limiting dilution assays to quantify the effect.
(4) On page 10, the authors used several primary cancer cell lines established in their lab. However, the status of Bmi-1 in those cells before and after compound treatment was not clearly presented.
(5) In Fig. 1a, the authors showed that CD49hCD29hCD44h cells express Bmi-1 at a higher level than the CD49lCD29lCD44l cells. Since the former cell population only constitutes a small fraction of total cells, how the authors explain that the Bmi-1 expression in total cells is the same as that in CD49hCD29hCD44h population?

Reviewer #2 (Remarks to the Author):

This is overall a well conceived, though rather sloppily put together, manuscript on a novel strategy to target prostate tumor initiating cells (TICs). Specifically, they have developed what appears to be selective inhibitors of translation of BMI-1, a component of the polycomb chromatin remodeling complex which is required for many attributes of prostate cancer TICs. The xenograft studies involving zebrafish and C49b-hi,CD29-hi, CD44-hi TICs, as well as secondary and tertiary spheroid formation studies provide decent evidence that targeting BMI-1 in TICs is a promising approach to treat advanced prostate cancers. However, there are a number of areas that need clarification and must be addressed.

Comments:
1) In the early section of the paper, DU145 PCa cells are used interchangeably with C49b-hi,CD29-hi, CD44-hi TICs. For instance, in Figure 1b and 1d, the figure legend states the data involves C49b-hi,CD29-hi, CD44-hi TICs, but the text states the data is for DU145 cell lines. Although DU145 and C49b-hi,CD29-hi, CD44-hi could be equivalent in certain contexts, there is no prior introduction as to how they are related, so I'm not sure which cells the experiments are referring to. Please clarify.
2) BMI-1 translational inhibitors are very interesting class of compounds, but the key is that they appear to target translation of BMI-1. While they do have dose-dependent effects on BMI-1 protein levels by ELISA, what is the mechanism of their action? Based on their effects on GAPDH levels and b-actin, b-tubulin, H2A, they appear to be somewhat selective, but could this be entirely due to differences in protein half-life? What is the half-life of BMI-1, and Mon-ubiquitinated H2A (gamma-H2A) in relation to GAPDH, b-actin, b-tubulin and H2A? Perhaps these compounds are general inhibitors of protein translation that have "selectively impact" on proteins with short half lives such as luciferase? It seems that BMI-1 half-life is only~40 minutes. I wonder if the authors could test the effects of these inhibitors on an unrelated cellular protein with equally short half-life. At minimum, it would be important know how long the cells were treated to determine BMI-1 protein levels
by ELISA and Westerns. This seems important given the proposed mechanism by which these compounds are thought to function.
3) What is the effects on luciferase reporter if the BMI-1 5'-UTR or 3'-UTR are mutated? That would suggest that the compounds' effect on BMI-1 translations is selective. I assume controls such as this were performed, but it's not described in the manuscript. Again, this control seems important given the proposed mechanism by which these compounds are thought to function.

4) On a related note, I wonder what the effects of a general translational inhibitor cyclohexamide (CHX)in this TIC model. Very strong evidence that the important biological effects of BMI-1 inhibitors are not due to general inhibition of translation would be if treatment with CHX does not impact secondary and tertiary spheroid formation (Figure 2c).
5) According to the authors, one of the most compelling evidence that BMI-inhibitor C-209 is selective for BMI-1 is that, at concentrations that inhibit xenograft tumor growth (2uM), there is little apparent toxicity to the zebrafish embryo when added at 12-hours post fertilization. At 10uM, however, there is what appears to be heart failure phenotype (as evidenced by what appears to be pericardial effusion) at 24 and 48-hpf, associated with moderate decreased survival at 48hpf. While this does not detract from the author's main thesis that effects of C-209 at 2uM is not due to nonspecific toxicity associated with general disruption in translation, a control data using cycloheximide (CHX) would bolster their argument. Such controls studies are important because the therapeutic window for C-209 appears very narrow.
6) Also, given such narrow therapeutic window for C-209 in embryos, what is the rate of death in xenograft studies. While some degree of mortality should be expected from the procedure itself, it would be important to see whether C-209 causes excess mortality over DMSO controls.
7) As a support of selectivity of BMI-inhibitor C-209, the authors mention lack of significant inhibition of a panel of 160 kinases and 21 phosphatases, but this would not be a definitive evidence for C-209 selectivity, especially since this is supposed to be a translational inhibitor. Also, in the procedures section, they state they used a 245-kinase panel. Please clarify this minor point.

Additional points:
8) Figure 6 d and 6e appeared to be reversed based on the figure legend.
8) Page 9: "...unlike C-209, both C-210 and C-211 exhibited adverse pharmacokinetic properties at later time points." The use of "Pharmacokinetic properties" here doesn't seem to match the traditional definition involving absorption, distribution and metabolism of specific drug in the body. Nowhere else in the manuscript does the authors examine the "pharmacokinetic properties," so further explanation is needed.
9) Figure 3 legend (Page 33): (a)... curling of the tail as in the panels associated with C-211 might represent dorsalization due to interference with embryonic stem cell developmental pathways." This statement is wrong - the dorsal curvature of tail does not represent dorsalization. Suggest the authors review genetic pathways that result in tail axial changes such as Notch pathway. And the statement that this may be due to "embryonic stem cell developmental pathways" doesn't make sense at all as embryonic stem cells as classically defined has not yet been identified in zebrafish. Please be more precise.
10) Page 9: "C209-additioned water" is awkward. Suggest "C209-containing egg water." I am assuming that the authors are not leaving the embryos in plain water.

Reviewer #3 (Remarks to the Author):

In this manuscript, the authors tested the hypothesis that BMI-1 is critically important for the initiation and progression of human prostate cancer and developed a new BMI-1 chemical inhibitor, which was shown to repress tumor progression and growth in both in vitro and in vivo models. Moreover, the authors demonstrated that the new inhibitor might be useful in targeting the tumor initiating cells. The data presented in this manuscript is interesting, but improvements are needed before it is ready for publication.

Major Points:

1. What is the mechanism for BMI-1 inhibition by the identified compounds, such as C-209? Do they directly inhibit BMI-1 translation? Do they inhibit BMI-1 at other stages, indirectly, or even through a mechanism that is independent of BMI-1?
2. Two of the three compounds were dismissed due to their toxicity in zebrafish embryos. However, embryos are different from adults and these compounds may not be toxic to adults. Is there data suggesting that these compounds are indeed toxic to adult animals?

Minor Points:

1. In multiple places in the text, e.g., line 4 of the second paragraph on page 5, and line 6 of the second paragraph on page 14, "PCa cells" or "TICs" were used to describe cells in an experiment. It should be stated clearly which PCa cells or TICs they are, whether they are primary tumor cells or cell lines. For cell lines, the name of the cell line should be given.
2. In figure 2c, MTX was more effective in inhibiting colony formation in secondary spheroids than in tertiary spheroids, while C-209 and C-211 were more effective in tertiary spheroids. Was this observation reproducible? What is the explanation for this difference?
3. In figure 3d human CD34+ hematopoietic cells were used as a control for the prostate cancer cell line DU145. CD34 cells are not the appropriate cell type to serve as controls for the DU145 cells.
4. The FACS data presented in figure 4c should be converted to bar graphs to show statistically significant changes in the cell populations after treatment.
5. In figure 6b-c, most fish embryos had major responses to C-209 treatment with drastically reduced tumor mass. Yet, in figure 6f, most of the treated embryos still contained enough tumor cells for secondary transplantation. Is there a discrepancy here?
6. More experimental details need to be provided for the mouse experiments. For example, what cell population (and how were they isolated and prepared) was used for clonogenic assay and serial transplantation described on page 15 and figure 7a?
7. What are the BMI-1 expression levels in the primary tumor cell samples listed in Table 1? Was there any correlation between BMI-1 expression level and the response to C-209 treatment?
8. Figure legends (all of them, including the supplemental ones) should include dosages of various compounds used.
9. The actual prostate cancer samples used in figure 4 should be named in the figure legend. For data in figure 4b and c, how many samples were tested? The last sentence in the figure legend, does it mean that "... from two independent experiments performed with cells derived from eight patients? If so, the graphs in these two panels represent 16 independent data points (8 patients x 2 experiments). Is this correct?
10. For figure 6 d (the figure legend is reversed) how was the tumorigenic capacity determined and calculated?
11. For figure 6f, how many TICs were injected per embryo?

Reviewer #4 (Remarks to the Author):

Bansal et al describes a screen for small molecules inhibiting Bmi1 translation. Identified molecules are then used to study the role of Bmi1 for propagation of prostate cancer tumor initiating cells (TICs) in vitro and in vivo. The role of Bmi1 for tumor growth and initiation is tested using old classical cell lines as well as patient-derived cells. A role of Bmi on these kinds of cells has been published before, so the new and interesting data is that of the compound.
General comments; the manuscript could be better organized and it is difficult to read and follow the logic of the experiments. In its present form and lacking some key data I am unable to fully judge whether the findings are of such magnitude to recommend publication. Thus, in the absence of clear in vivo data documenting the potency and efficiency of the compound it is difficult to be positive. Furthermore, it is sometimes unclear what cells, concentration and time are used, even after searching through both
materials and methods and figure legends. This has to be fixed throughout the manuscript.
Very little effort is made to understand the mechanism of the compound.
1) How does it block Bmi1? Here there is a lack experiment trying to understand what the compound actually is doing, what the targets of interactions are and how selectivity to Bmi1 in prostate cells is achieved. Perhaps one cannot expect all these issues to be solved, but at least some could have been addressed and/or discussed.
2) What happens to cells with blocked Bmi1? There are contradictory results on this issue, showing a senescence effect in one experiment, reduced proliferation in other experiments and finally cell death in yet other sets of experiments. These are very straightforward experiments which can be systematically approached in its own figure instead of being scattered throughout the manuscript. I think that for a journal of this quality a systematic approach to these questions can be requested.
3) Is the mechanism fully dependent/mediated via Bmi1? For instance, what is the IC50 of cells with Bmi1 RNAi as

compared to control cells? Similar such key experiments conclusively linking C-209 compound via Bmi1 to its effects on prostate cancer cells is needed.
The molecule is very similar to a molecule described by James Chen lab (Cupido et al., DOI: 10.1002/anie.200805666) which acts on microtubule and hedgehog signaling. So Bmi1 may not be the only target of this molecule.
4) The selective effect on stem cell/TICs is not convincing. It seems that nearly all cells die/disappear in just a few days in the dose response MTS viability assay. Since the TIC population is expected to be relatively small, it seems the compound acts also on other tumor cells. This issue could easily have been addressed comparing TIC enriched vs remaining cells in the IC50 viability assay and other rapid and simple assays. Based on both the in vitro and in vivo data, it seems to me that effects are on prostate cancer cells in general, but also including the TIC population which are partly refractory to general cytostatic. Hence, a more general effect does not alter the overall conclusion, but this issue needs to be accommodated in the manuscript text.

5) "Effect of Bmi1 inhibition on normal stem cells" This title is inadequate as toxic effects on Zebrafish larvae are studied. If effects on stem cells are studied, they should have determined the IC50 on ESCs, neural stem cells and other stem cells.
6) Adequate quantification is missing on some experiments, for instance Fig 4c.
7) In the motility assay, is this experiment normalized for death of cells? Hence, the reduced effects on motility could be secondary to that most cells die.
8) Please clarify in main text how compound was administered to Zebrafish.
9) Only percent Zebrafish responders are presented, but not how good the response is. This data would be significantly strengthened if quantification of tumor size/volume was quantified. It is not clear exactly which patient-derived tumor cells were used in these experiments. Were it the same as in other experiments or from a different patient?
10) Figure 7b provides the key data for this manuscript. In this experiment only one data point shows significance. It would have been interesting to see further data points to substantiate this finding.
11) What is the relation between IC50 and inhibition of Bmi1?
12) In figure 5 at the top, it states "small molecule screen..." This is not a screen as far as I can understand.